



**OPPORTUNISTIC ACCESS IN FREQUENCY HOPPING
COGNITIVE RADIO NETWORKS**

THESIS

Ethan S. Hennessey, Captain, USAF

AFIT-ENG-14-M-38

**DEPARTMENT OF THE AIR FORCE
AIR UNIVERSITY**

AIR FORCE INSTITUTE OF TECHNOLOGY

Wright-Patterson Air Force Base, Ohio

DISTRIBUTION STATEMENT A:
APPROVED FOR PUBLIC RELEASE; DISTRIBUTION UNLIMITED

The views expressed in this thesis are those of the author and do not reflect the official policy or position of the United States Air Force, the Department of Defense, or the United States Government.

This material is declared a work of the U.S. Government and is not subject to copyright protection in the United States.

AFIT-ENG-14-M-38

OPPORTUNISTIC ACCESS IN FREQUENCY HOPPING
COGNITIVE RADIO NETWORKS

THESIS

Presented to the Faculty
Department of Electrical and Computer Engineering
Graduate School of Engineering and Management
Air Force Institute of Technology
Air University
Air Education and Training Command
in Partial Fulfillment of the Requirements for the
Degree of Master of Science in Electrical Engineering

Ethan S. Hennessey, B.S.E.E.

Captain, USAF

March 2014

DISTRIBUTION STATEMENT A:
APPROVED FOR PUBLIC RELEASE; DISTRIBUTION UNLIMITED

OPPORTUNISTIC ACCESS IN FREQUENCY HOPPING
COGNITIVE RADIO NETWORKS

Ethan S. Hennessey, B.S.E.E.
Captain, USAF

Approved:

//signed//
Kenneth M. Hopkinson, PhD (Chairman)

28 Feb 2014
Date

//signed//
Robert F. Mills, PhD (Member)

28 Feb 2014
Date

//signed//
Maj Mark D. Silvius, PhD (Member)

28 Feb 2014
Date

Abstract

Researchers in the area of cognitive radio often investigate the utility of dynamic spectrum access as a means to make more efficient use of the radio frequency spectrum. Many studies have been conducted to find ways in which a secondary user can occupy spectrum licensed to a primary user in a manner which does not disrupt the primary user's performance. This research investigates the use of opportunistic access in a frequency hopping radio to mitigate the interference caused by other transmitters in a contentious environment such as the unlicensed 2.4 GHz region. Additionally, this work demonstrates how dynamic spectrum access techniques can be used not only to prevent interfering with other users but also improve the robustness of a communication system.

Table of Contents

	Page
Abstract	iv
Table of Contents	v
List of Figures	vii
List of Tables	ix
List of Acronyms	x
I. Introduction	1
1.1 Problem Statement	2
1.2 Contributions	2
1.3 Overview	3
II. Background	5
2.1 Related Work	6
2.2 Frequency Hopping Spread Spectrum	8
2.3 Spectrum Sensing	9
2.4 Radio Environment Map	11
2.5 Wireless Open-Access Research Platform	11
III. Methodology	13
3.1 Approach	13
3.2 System Boundaries	14
3.3 System Services	14
3.4 Workload	16
3.5 Performance Metrics	18
3.6 System Parameters	18
3.7 Factors	20
3.8 Evaluation Technique	20
3.9 Experimental Design	23
3.10 Modem Operation	24
3.11 Methodology Summary	25

	Page
IV. Results	27
4.1 Simulation Results	27
4.1.1 Model Validation	27
4.1.1.1 frequency shift keying (FSK) Baseline	27
4.1.1.2 frequency hopping (FH) Baseline	29
4.1.1.3 Spectrum Sensor	31
4.1.2 Dynamic spectrum access (DSA) Performance	31
4.1.2.1 Single Tone Interference	32
4.1.2.2 Multi-tone Interference	36
4.1.2.3 Wideband Interference	40
4.2 Hardware-in-the-Loop Results	44
4.2.1 Validation and Baseline Performance	45
4.2.2 DSA Performance	46
V. Conclusions	50
5.1 Summary	50
5.2 Future Work	52
Appendix: WARPLab Function Library	54
References	56

List of Figures

Figure	Page
2.1 Cognitive radio system functional diagram.	7
3.1 Opportunistic frequency hopping modem.	15
3.2 System functional block diagram.	16
3.3 Hop set selection function model.	22
3.4 Transmitter function model.	23
3.5 Receiver function model.	23
3.6 WARPLab functional diagram.	24
4.1 Baseline M -FSK performance (without filters).	28
4.2 Baseline M -FSK performance (with filters).	29
4.3 Baseline FH performance (without interference).	30
4.4 Baseline FH performance (with interference).	31
4.5 Demonstration of spectrum sensor identifying four interfering tones.	32
4.6 Non-adaptive bit error rate (BER) performance as a function of interference to signal ratio (ISR) with one interfering tone present.	33
4.7 Non-adaptive BER performance as a function of E_B/N_0 with one interfering tone present.	34
4.8 Adaptive BER performance as the spectrum sensing rate increases relative to the environment change rate with one tone interferer.	35
4.9 Throughput of FH spread spectrum (FHSS) system for multiple ratios of spectrum sensing rate to environment change rate with one tone interferer present.	36
4.10 Non-adaptive BER performance as a function of ISR with multiple interfering tones present.	37

Figure	Page
4.11 Non-adaptive BER performance as a function of E_B/N_0 with multiple interfering tones present.	38
4.12 Adaptive BER performance as the spectrum sensing rate increases relative to the environment change rate with multiple tone interferers.	39
4.13 Throughput of FHSS system for multiple ratios of spectrum sensing rate to environment change rate for 2, 4, and 8 tone interferers present.	40
4.14 Non-adaptive BER performance as a function of ISR with orthogonal frequency-division multiplexing (OFDM) interference present.	41
4.15 Non-adaptive BER performance as a function of E_B/N_0 with OFDM interference present.	42
4.16 Adaptive BER performance as the spectrum sensing rate increases relative to the environment change rate with OFDM interference.	43
4.17 Throughput of FHSS system for multiple ratios of spectrum sensing rate to environment change rate with one tone interferer present.	44
4.18 Baseline hardware-in-the-loop (HIL) FSK performance.	45
4.19 Baseline HIL FH performance.	46
4.20 Non-adaptive HIL BER performance as a function of ISR with one interfering tone present.	47
4.21 Non-adaptive HIL BER performance as a function of E_B/N_0 with one interfering tone present.	48
4.22 Adaptive HIL BER performance as the spectrum sensing rate increases relative to the environment change rate with one tone interferer.	49
4.23 Throughput of FHSS system for multiple ratios of spectrum sensing rate to environment change rate with one tone interferer present.	49

List of Tables

Table	Page
2.1 Select themes from Air Force science and technology vision.	6
3.1 Experimental factors and levels.	21
3.2 FHSS simulation design parameters.	26
4.1 ISR required to increase BER by one order of magnitude over baseline performance of 1.7×10^{-4}	38

List of Acronyms

Acronym	Definition
AFIT	the Air Force Institute of Technology
AWGN	additive white Gaussian noise
BER	bit error rate
CR	cognitive radio
CRN	cognitive radio network
CUT	component under test
DARPA	the Defense Advanced Research Projects Agency
DSA	Dynamic spectrum access
FFT	fast Fourier transform
FH	frequency hopping
FHSS	FH spread spectrum
FM	frequency modulation
FPGA	field-programmable gate array
FSK	frequency shift keying
HIL	hardware-in-the-loop
IEEE	Institute of Electrical and Electronics Engineers
IF	intermediate frequency
ISR	interference to signal ratio
LAD	localization algorithm based on double-thresholding
MA	multiple access
MFSK	M -ary frequency shift keying
MIMO	multiple-input/multiple-output
OFDM	orthogonal frequency-division multiplexing

Acronym	Definition
PN	pseudo noise
PU	primary user
PSD	power spectral density
PSK	phase-shift keying
REM	radio environment map
RF	radio frequency
ROC	receiver operating characteristic
SDR	software defined radio
SINR	signal to interference plus noise ratio
SNR	signal to noise ratio
SU	secondary user
SUT	system under test
USAF	United States Air Force
WARP	Wireless Open-Access Research Platform
WRAN	Wireless Regional Area Network

OPPORTUNISTIC ACCESS IN FREQUENCY HOPPING COGNITIVE RADIO NETWORKS

I. Introduction

IT is an uncontested assertion in the field of communications that the radio frequency spectrum is overcrowded in the United States and around the world. Fortunately, it is also true that the spectrum is under-utilized considering other various domains (spatial, temporal, etc.). Making more efficient use of the spectrum available is a principal contribution sought by researchers in the field of cognitive radio (CR). Dynamic spectrum access (DSA) is a key enabling technology that continues to be developed and refined to achieve this purpose. DSA refers to a range of concepts and technologies aimed at allowing an unlicensed secondary user (SU) to occupy spectrum belonging to a licensed primary user (PU) in a manner that does not interfere with PU operation. DSA techniques generally fall into one of two categories of implementation. The first is *spectrum underlay* whereby the SU transmits in the licensed band occupied by the PU in a manner which does not disrupt the PU. In the second technique, known as *spectrum overlay*, the SU only uses the licensed spectrum when the PU is not transmitting. Spectrum overlay is often referred to as *opportunistic access*.

CR is first introduced to the field in 1999 by Dr. Joseph Mitola who presents a significant expansion of his previous vision for software defined radio (SDR) [1]. This vision includes a model of SDR self-learning to encompass awareness of self, neighboring networks and nodes, and even applications and transmission medium. In 2005, the topic of CR is picked up by Dr. Simon Haykin. In his work, Haykin provides a seminal survey of CR to that point and focuses the trajectory of research on two primary objectives. These

objectives are to provide “highly reliable communication whenever and wherever needed” and “efficient utilization of the radio spectrum” [2]. This work coincides with a tremendous increase in attention on CR. Recently, much of the research in DSA has been focused on techniques by which an unlicensed SU can detect the availability of spectrum that is unused by the licensed primary user, operate in the spectrum, and vacate the spectrum prior to inducing an appreciable level of interference when the primary user does resume operation. The Institute of Electrical and Electronics Engineers (IEEE) 802.22 Wireless Regional Area Network (WRAN) standard is a notable example of this access model. However, it should also be clear that DSA can be employed in unlicensed (or otherwise contentious) spectrum to reduce the impact of interference to a user’s own communication system.

1.1 Problem Statement

The objective of this research is to develop and implement an experimental frequency hopping (FH) modem prototype that leverages limited knowledge of the local spectral environment for opportunistic access in a contentious environment. The prototype is implemented through both simulation and hardware-in-the-loop (HIL) testing. The resulting models are used to characterize the efficacy of implementing opportunistic access for interference mitigation. It is expected that, given some knowledge of the spectral environment, communication performance can be improved by rapidly adapting the transmitted waveform to suit the environment.

1.2 Contributions

This research provides the following contributions:

1. *A prototype modem for future work by the the Air Force Institute of Technology (AFIT) CR team.* At the time this research began, the AFIT CR team had no working CR with which to perform testing. The hardware platform had been

identified and many of the essential functions had been designed and demonstrated. Upon the integration of the prototype modem presented here with the past work discussed in Chapter 2, the AFIT CR team will have a radio capable of repeating cycles of the observe, orient, decide and act (OODA) loop thereby demonstrating a rudimentary level of cognition.

2. *Performance analysis of an opportunistic FH modem in the presence of interference.* This research explores the robustness of a FH modem to reject interference when given the capability to sense the presence of interference and adapt the communication waveform.
3. *Library of WARPLab utility functions to speed development of future prototyping efforts.* Much of the software developed to produce and test the prototype modem was constructed with modularity in mind. The scripts and functions can easily be used in future prototyping efforts that use WARPLab. A description of these modules is included in the appendix.

1.3 Overview

Chapter 2 discusses recent and ongoing research related to the implementation of opportunistic access in FH networks. Additionally, topics related to the functionality of the radio network are introduced. These concepts provide a foundation for many of the decisions for the experimental design in Chapter 3.

Chapter 3 formally introduces the hypothesis driving this research. It then describes the design and functionality of the prototype fast FH modem used to evaluate the hypothesis. This chapter also discusses the parameters and boundaries of the experiments and results. Finally, relevant factors and levels are discussed along with the design of experiments.

Chapter 4 provides detailed results on the outcomes of the experiments described in Chapter 3. Where applicable, comparisons are made between theoretical, simulated, and direct measurement performance. Statistically based observations are made to describe system performance in accordance with the metrics collected on each configuration.

Chapter 5 summarizes experimental results with additional analysis and discusses implications of results. An overall evaluation of the experimental modem's performance based on the data obtained is provided. The conclusion is that, for the experimental parameters chosen, the probability of bit error is not increased by implementing DSA and is in some cases improved. In all experiments, however, the overall throughput of the system is the same or worse. Finally, relevant topics for future work are discussed.

II. Background

DUE to the scarcity of spectral resources—particularly in densely populated areas—many communications researchers have turned their attention to the area of DSA as a solution. DSA has potential to alleviate spectrum congestion by allowing SUs to transmit either when the PU is not or in a manner which does not appreciably degrade performance of the PU. In addition to the generic desire to improve efficiency and reliability of digital wireless communications, the CR research team at AFIT is motivated by the strategic technological vision laid out by the United States Air Force (USAF) chief scientist in [3]. The strategic study presents twelve overarching themes intended to keep the USAF in the technological forefront of worldwide military operations through the next decade. The AFIT CR research team endeavors to advance military communications in regards to six of these themes. These six themes are listed in Table 2.1¹ with attention drawn to entries that are particularly relevant to this document. In 2012, the Defense Advanced Research Projects Agency (DARPA) began a project seeking to conduct “advanced radio frequency (RF) mapping” to provide military commanders a “RadioMap” of the battlespace [4]. The desired result is to alleviate the spectrum congestion caused by the numerous communications requirements that exist in today’s complex military operating environments.

CR technologies promise to deliver benefits other than spectral efficiency as well. For instance, Self-organizing networks offer to reduce the complexity (from a user perspective) in managing large networks [5]. This document, however, will be limited to focusing on a method to reduce the impact of interference in a unlicensed region of spectrum. Additionally, unless otherwise stated, the term DSA may be assumed hereafter to refer to the particular method of spectrum overlay described in this document.

¹Partially reproduced from [3]

Table 2.1: Select themes from Air Force science and technology vision [3].

From decreased emphasis on this...	To increased emphasis on this...	Relevance
From...Fixed	To...Agile	Primary
From...Control	To...Autonomy	Secondary
From...Preplanned	To...Composable	N/A
From...Single domain	To...Cross domain	N/A
From...Permissive	To...Contested	Primary
From...Sensor	To...Information	Secondary

The following sections discuss related work and constituent technologies that are relevant to this research.

2.1 Related Work

CR has been identified in numerous publications as a means to achieve more efficient use of the radio spectrum than is currently possible with the licensed PU model. Many techniques have been proposed to permit unlicensed SUs to opportunistically take advantage of underutilized licensed spectrum [6]. AFIT has developed the following model as a framework to create a DSA cognitive radio network (CRN). Figure 2.1² is a system functional diagram as introduced in [7]. In state O-1 each CR ceases transmission to sense the RF environment and in state O-2 network partitions (or “clusters”) are formed. These clusters are to aid in managing overhead associated with other states in the cycle. With each CR contributing its knowledge of the available spectrum (i.e. spectrum maps) in state O-3, a composite map is created in state O-4. The merged map data is used to determine a waveform commonly suitable to each participating CR in state O-5. The resulting waveform (or its defining characteristics) is finally distributed in O-6 then

²Reproduced from [7]

utilized in O-7 until conditions dictate another iteration of the process. States O-4 and O-5 are specifically addressed in [8] where the authors implement map merging and adaptive hopset selection (in the form of FH) on an field-programmable gate array (FPGA). In [9] the same author addresses the forming of network partitions via a k -means clustering algorithm based on spectral and spatial proximity.

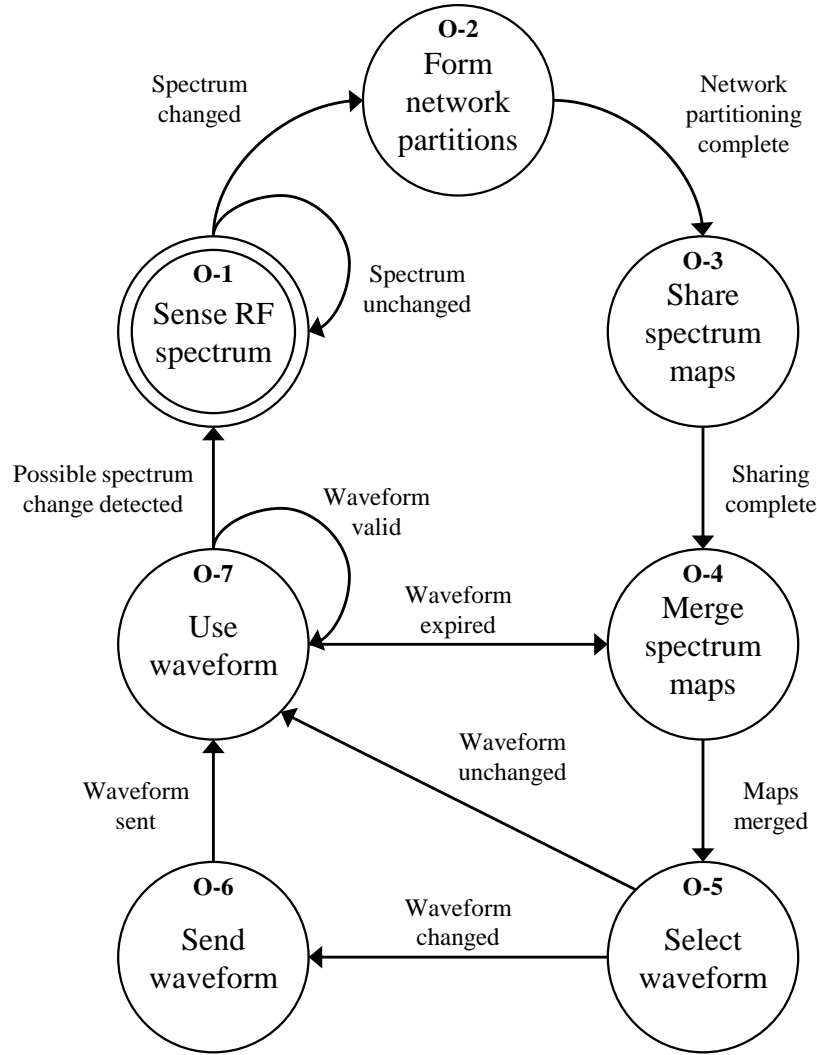


Figure 2.1: Cognitive radio system functional diagram.

2.2 Frequency Hopping Spread Spectrum

Spread spectrum communication is a collection of techniques used to “spread” an otherwise narrowband signal such that the resulting waveform spans a relatively wide frequency band. In general, spread spectrum technologies are useful in reducing the impact of interference on a communication system. It is also possible to design a spread spectrum system to accommodate multiple access (MA) users, allowing multiple transmitters to occupy the same region of RF spectrum with minimal mutual interference.

FH spread spectrum (FHSS) is form of spread spectrum where a narrowband communication signal “hops” over a specified pseudo noise (PN) sequence of transmit channels within some wider bandwidth. Each hop is of a fixed duration in time and only occupies one transmit channel at a time. In most FHSS systems each transmit channel is equally probable in the sequence. The resultant power spectral density (PSD) over time is nearly rectangular and spans the entirety of the spread spectrum bandwidth. In some publications, a hop is referred to as a *chip*. In this document, hop, when used as a verb refers to the act of changing frequencies. When used as a noun, hop refers to a slice of frequency spectrum while chip refers to a slice in time. Due to the relationship of these terms, they are often used interchangeably.

It is possible to further increase the robustness of a FHSS system by selecting a chip rate greater than the symbol rate. Increasing the chip rate over the symbol rate adds *frequency diversity* and reduces the probability that an interfering source will cause a decision error for a given symbol. This is known as *fast frequency hopping* and allows for two intervals in which symbol detection may occur.

The first method is chip-by-chip detection where a hard decision is made on each chip and the final chip decision is based on a majority rule. For this reason it is common to use an odd number of chips per symbol since adding an additional chip would not increase the information with which to make a decision but would increase the probability of

making a symbol error [10]. If signal to noise ratio (SNR) is sufficiently high and the power of an interferer in a particular transmit channel is high enough to force a chip error, [10] provides the closed form approximation

$$P_e = \sum_{x=r}^c \binom{c}{x} p^x (1-p)^{c-x}, \quad (2.1)$$

where p is the probability of error for a single trial, c is the number of chips per symbol and r is the number of wrong chip decisions needed to result in a symbol error.

The second method of detection is to make a symbol-by-symbol decision. In this method each chip is synthesized back to baseband and concatenated with the remaining constituent chips for a single decision on the entire symbol. This method performs better in noise; however, interference in one chip impacts the entire symbol. The result is slightly poorer performance in the presence of interference when compared to chip-by-chip detection.

2.3 Spectrum Sensing

Spectrum sensing is the essential enabling process necessary to support DSA for the prototype modem in this research. It is the process by which detailed localized data is provided for the radio environment map (REM) which is introduced in Section 2.4. Spectrum sensing is also key to constructing the PN sequence used for FH. Multiple taxonomies have been introduced seeking categorize the numerous spectrum sensing techniques [11–13]. For the purposes of this document, spectrum sensing is divided into the following categories:

- *Energy detection* is the most straight forward form of spectrum sensing. It is easy to implement and requires no knowledge of PU signal structure. It is, however, not very robust in detecting signals near the noise floor due to susceptibility to noise uncertainty [14]. Energy detection pays no regard to signal structure and considers only the energy magnitude contained in some bandwidth. For SUs chiefly

concerned with identifying and avoiding interfering with the transmissions of a PU, energy detection can be problematic. The authors of [15] simulate and demonstrate a method of energy detection referred to as localization algorithm based on double-thresholding (LAD) using the Wireless Open-Access Research Platform (WARP) which is introduced in Section 2.5 [16].

- *Matched filtering* is frequently cited in the literature as providing the optimal solution for detecting the presence of PUs for which the signal structure is known. The authors of [17] demonstrate the resilience of the matched filter to noise uncertainty. Unfortunately, this method provides very little utility if the PU signal does not resemble a reference signal known to the spectrum sensor.
- *Feature detection* refers to a class of sensing methods which use some form of statistical analysis of the sampled spectrum. Examples of feature detection include cyclostationary feature detection [18], time covariance based detection [19], and eigenvalue-based detection [20]. Each of these methods are more robust than energy detection and do not require *a priori* knowledge of the PU signal structure; however, they come at a cost of significantly increased complexity. This complexity drives not only higher development costs, but also more expensive and larger devices which is problematic for mobile communication devices.

The receiver operating characteristics (ROCs) of each of the previously mentioned categories are compared in [21]. The results demonstrate how the deficiencies of energy detection and matched filtering compare to cyclostationary feature detection. Since this research is only concerned with avoiding interference for the purpose of improving performance, energy detection is a sufficient method of spectrum sensing for the following experiments.

2.4 Radio Environment Map

Another fundamental concept related to this research is the idea of the REM. The REM is first introduced in [22] as a means to manage resources available to WRANs. In the authors' original vision the REM is described as an integrated database which contains "multi-domain environmental information, such as geographical features, available services, spectral regulations, locations and activities of radios, relevant policies and past experiences" [22]. This concept has gained considerable traction and has been further developed to include the notion of *global*- and *local-REM* [23]. This delineation helps to address resource allocation among peer networks and create a hierarchy to support focused sensing strategies. The relevance of this hierarchy is demonstrated in [24] where the authors show a point of diminishing returns as the number of sensors in a CRN increases. Researchers have explored the construction of REMs in [25–27]. In addition to collecting the local spectrum data, it is necessary to share the data among networks and nodes. In [28], the authors demonstrate an emulation environment to evaluate the reliable dissemination of REM information through totally ordered multicast. AFIT is also pursuing the research of algorithms and protocols to support utilizing shared REM data in network rendezvous [29].

2.5 Wireless Open-Access Research Platform

Several experimental SDR design platforms are available for today's researcher. In addition to the flexibility of software definition, it is also desirable for the research platform to support *firmware* definition [30]. Among this class of radio, platforms feature an FPGA to provide a high level of reconfigurability as well as offering the efficiency of hardware design. A brief discussion of the available platforms as well as the reason for AFIT's selection are provided in [8].

To conduct hardware research, AFIT has selected the WARP v2 designed by Rice University. WARP provides a Xilinx Virtex FPGA based design featuring a PowerPC

general purpose processor and support for multiple-input/multiple-output (MIMO) communications. Along with an open-source community and multiple reference designs, WARP features the powerful WARPLab which provides for fast physical- and link-layer prototyping with MATLAB [16].

III. Methodology

THE objective of this research is to determine the efficacy of DSA (or opportunistic access) for interference mitigation. Specifically, the following research questions are asked:

- Can interference mitigation in a fast FH radio network be further improved by leveraging the capability of DSA?
- How does bit error rate (BER) increase or decrease given various interference profiles when compared to a non-adaptive FH radio?

In response, the following hypotheses are formed:

- **Hypothesis 1:** *As knowledge of interference increases in accuracy and approaches real time, BER will approach optimal performance for a given SNR.*
- **Hypothesis 2:** *BER performance of an opportunistic FH radio network is not worse than that of a fixed sequence FH network in the presence of interference.*

3.1 Approach

This evaluation looks specifically at DSA in a fast FH radio network. Fast frequency hopping—where the chip (frequency hop) rate exceeds the symbol rate—is selected for the so called “frequency diversity” observed for each transmitted communication symbol [31]. System performance is evaluated with respect to BER given various interference profiles such as partial-band and multi-tone interference. Performance is compared for the same system given two configurations: a control configuration employing a static PN sequence to determine the carrier frequency and a configuration leveraging spectrum sensing to identify and avoid the presence of interference. Both configurations are modeled in MATLAB with simulated results compared to the theoretical bit error rate

expression for FH spread spectrum systems. A subset of the simulation experiments are executed in HIL testing to provide a limited hardware comparison.

3.2 System Boundaries

The system under test (SUT) is an opportunistic FH modem which consists of a transmitter and receiver pair and the channel they communicate over. It is a physical (PHY) layer only model and therefore does not consider frames, protocols, or other higher layer attributes. The particular component under test (CUT) is the PN sequence generator. The operation of the system is described in Section 3.8. The scope of this experiment is to determine the impact that dynamically adapting a transmitted waveform has on receiver performance. The process synchronization between the transmitter and receiver are excluded from this study. Additionally, data formatting and source encoding are excluded to better understand the fundamental impact of the interference avoidance method. Figure 3.1 depicts the SUT along with the workload parameters, system parameters, services and metrics. Figure 3.2 provides a high level functional view of system operation. In the transmitter, the input data bits are modulated to M -ary frequency shift keying (MFSK) symbols prior to entering the FH modulator and ultimately the channel. The receiver follows this process in reverse and both the transmitter and receiver use the same spectral sensing process and PN sequence generation process as an input to the FH modulation/demodulation component.

3.3 System Services

Considering the transmitter/receiver pair, the SUT provides two services: transmission of digital information (bits) and estimation of received digital information. At a high level, transmission is achieved by mapping one or more bits to a communication symbol. This symbol is modulated as a physical waveform to be broadcast over a wireless channel. The process results in one of $M = 2^l$ symbols being transmitted where l is the

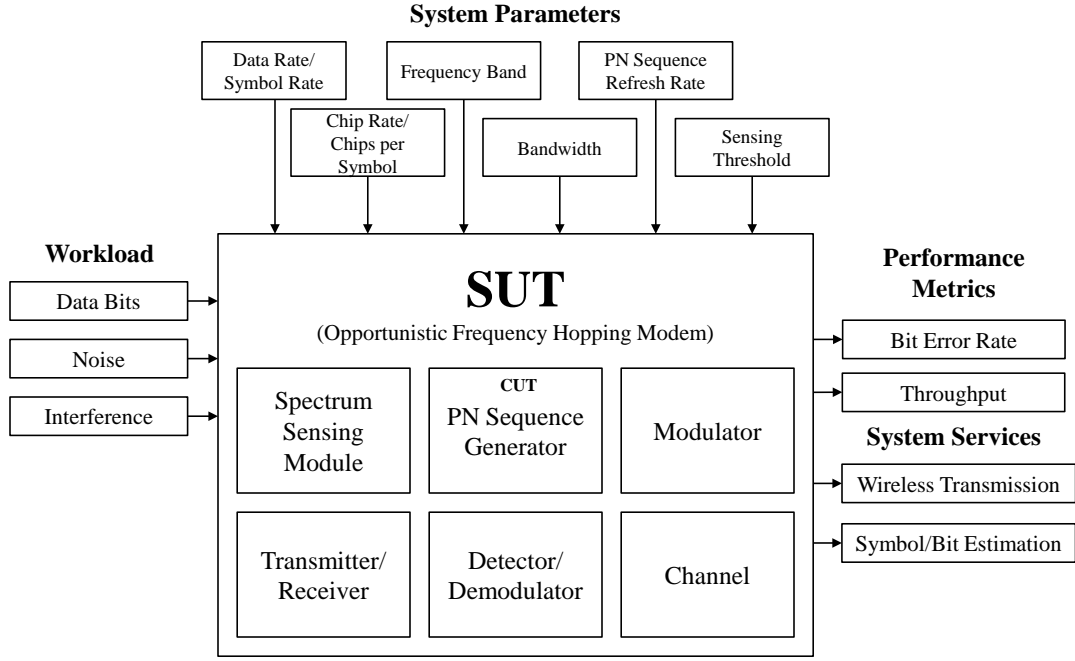


Figure 3.1: Opportunistic frequency hopping modem.

number of bits per communication symbol. Regardless which of M symbols is transmitted, the outcome is correct (i.e., the correct symbol is transmitted given the constituent input bits). On the receiver side, each received symbol goes through a detection process to estimate which of the M possible symbols was transmitted. The estimated symbol is demodulated and mapped to the appropriate estimated bits. The outcome of this process is zero to l bit errors per received symbol. The number of bit errors (given a symbol error) is dependent on how bits are mapped to symbols and which symbol was estimated.

The CUT (the PN sequence generator) provides a critical service to the SUT as well. The sequence generator is responsible for determining the set of frequencies the communication system can hop over. In the baseline configuration this set is fixed; however, in the experimental configuration this hop set changes periodically with the

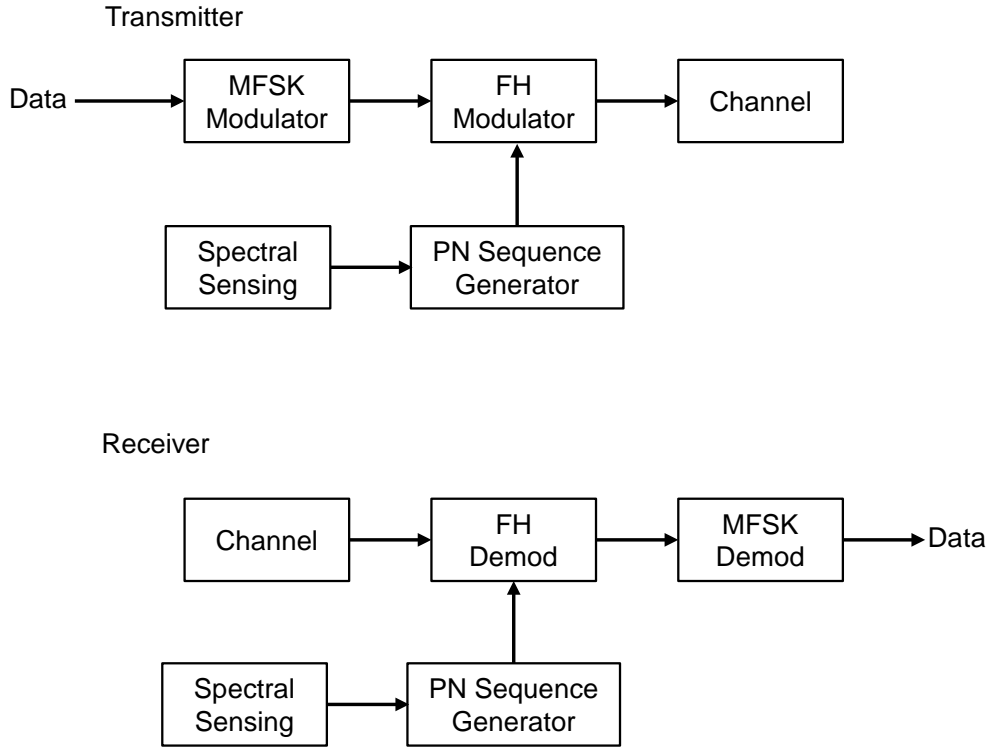


Figure 3.2: System functional block diagram.

dynamic spectral environment. The outcome of this service is to determine for each slice of the total available bandwidth whether or not the portion of spectrum is available. Depending on the spectrum sensing process, this could have varying degrees of accuracy. For this experiment, the sensing process (energy detection) is assumed to be perfect in simulation (i.e. at the time of spectrum sensing the resultant REM is correct given the sampled spectrum). Since the sensing process does not occur synchronously with respect to the dynamic spectral environment, the accuracy of sequence generation with regard to operation over available channels changes over time.

3.4 Workload

The system workload consists of three inputs: the modulated signal of interest, noise, and interference.

1. The signal of interest is simply a random binary waveform which is modulated using Gray³ coded MFSK. Signal power is varied to achieve desired power ratios (i.e., SNR and signal to interference plus noise ratio (SINR) or interference to signal ratio (ISR)).
2. The noise is an additive white Gaussian noise (AWGN) channel. In simulation noise is pseudo-randomly generated with noise power varied to achieve desired power ratios. In hardware, noise is dependent on the ambient environment. In test cases where the ambient noise is not approximately normal, AWGN is introduced in the receiver to preserve comparability between simulation and HIL results to the maximum extent possible.
3. The interfering signal varies in both power and shape. Three distinct interference profiles are presented in the workload⁴.
 - (a) Single tone interference - In this model a single narrowband sinusoidal tone is transmitted within some portion of the receiver bandwidth. The single tone interferer only affects one FH channel at a time. The FHSS system must be communicating on the impaired channel to be impacted at all.
 - (b) Multi-tone interference - Each tone in the model is a narrow-band signal capable of disrupting a single frequency hop in the set. Here each tone has the same structure as one of the M transmitted symbol and is therefore potentially recognized by the receiver to be the signal of interest.
 - (c) Structured wideband interference - Wideband interference is noise-like in the sense that it spans the bandwidth of the receiver RF front end filter. The signal is, however, structured and presents a different affect to the receiver. The

³Gray coding is a form of symbol assignment that results in the fewest bit errors given the most probable symbol errors.

⁴Each of the three interference profiles are derived from the models in [31].

signals are also often transmitted intermittently. An example of this type of interference is the bursty noise-like signal response characteristic of many orthogonal frequency-division multiplexing (OFDM) implementations, including some implementations of the IEEE 802.11 standard.

3.5 Performance Metrics

The principle measure of reliability in digital communication systems is the probability of bit error or BER [32]. BER is typically expressed as a function of some ratio of power or energy such as SNR or SINR. While other common performance metrics address considerations such as bandwidth efficiency or processing gain, they are not of particular interest and are therefore excluded from this experiment.

Ultimately, designers of most communication systems want to maximize the quantity of data the system can transmit and process. This is measured as the throughput of the system. For the purposes of this research, throughput is defined as

$$Throughput = \frac{\text{Number of bits transmitted} - \text{number of errors}}{\text{Number of bits transmitted} \times \text{Symbol duration}}, \quad (3.1)$$

and is expressed in bits per second.

3.6 System Parameters

The following parameters are known to impact the performance of digital communication systems.

1. *Data/symbol rate* - Data rate, R_D , measured in transmitted bits per second and symbol rate, R_S , measured in transmitted symbols per second, are fundamentally related by the relationship $R_D = lR_S$. The symbol rate drives the baseband bandwidth. Alternatively, bandwidth constrains the maximum symbol rate.

Generally, in frequency shift keying (FSK) systems, increasing the number of bits per symbol increases the data rate and reduces⁵ the theoretical BER.

2. *Chip rate* - In FHSS, the chip rate, R_C , determines the dwell time in a particular frequency hop. When $R_S > R_C$, multiple symbols (and therefore bits) are transmitted in a single chip. When $R_S < R_C$, frequency diversity is gained. This allows for a majority rule detection process where one or more hops are interfered with and the correct decision may still be made.
3. *System bandwidth* - The overall system bandwidth (measured in Hertz) in a FHSS determines the number of channels available in selecting a sequence (or hop set). It is possible to design a FHSS system with hops of overlapping bandwidth; however, in this work all hops are adjacent.
4. *Frequency band* - The operating frequency band plays a significant role in terms of policy constraining transmit power and bandwidth. Additionally, the frequency band can have a significant impact wave propagation. In general, as frequency increases, so does path loss. The shorter wavelength also results in greater signal attenuation due to obstructions and multipath reflection.
5. *Sensing threshold* - The thresholding technique and level used in the spectrum sensing process has a significant impact on the probability of correctly identifying the presence of another user in a channel.
6. *PN sequence refresh rate* - For opportunistic access to maximize its efficacy it is very important that the REM constructed by the sensing process be current. As the REM becomes stale in the dynamic environment, it is likely that the system will

⁵This is in contrast to the more common phase-shift keying variants in which an increase in modulation order results in an increased BER [33].

communicate on occupied channels while missing the opportunity to use unoccupied channels.

3.7 Factors

From the list in Section 3.6, the parameter most unique to this experiment is the PN sequence refresh rate. The workload factors (i.e. interference profiles) and PN sequence refresh rate are captured with their levels in Table 3.1.

1. Refresh rate - It is expected that as the refresh rate increases, the BER will tend towards that of a channel where no interference (other than noise) is present and as the refresh rate decreases, the BER will tend towards that of the control configuration. The refresh rate is represented as the ratio of spectrum sensing to the rate of environment change. This ratio is considered over eight logarithmically scaled levels from 0.01 to 100.
2. Interference profile - The structure of the interference is expected to impact the modems resiliency to avoid the impediment and reduce BER. The three interference profiles discussed in Section 3.4 will be broken down to five levels (three of which are the multi-tone profile) in simulation with just the single tone profile considered in hardware.

3.8 Evaluation Technique

The system itself is conceptually modeled based on development in [34] with DSA elements influenced by [15] and [35]. The model is constructed and simulated in MATLAB 2012b. The baseline simulation performance is validated against theoretical BER expressions for FHSS derived in [10]. Simulation is selected for the evaluation technique as a practical first step before committing expensive and time consuming resources toward direct measurement on physical systems.

Table 3.1: Experimental factors and levels.

Factor	Level	
Ratio of spectrum sensing to environment change	0.01	1.93
	0.037	7.20
	0.139	26.8
	0.518	100
Interference Profile	Single Tone	
	Multi-tone	{2, 4, 8}
	Wideband	

The MATLAB model consists of three primary functions. The first is the hop set generator shown in Figure 3.3. This function periodically samples the noise, $n(t)$, and interference, $i(t)$, present in the system bandwidth and applies a fast Fourier transform (FFT) to create a REM. The PN sequence generator then uses a simple threshold on the FFT to create a binary vector indicating which channels are available for transmission. The threshold is user definable in absolute power or relative to observed ambient mean power. This binary vector is used to constrain the available frequencies selected for the PN sequence. The output of this function is the vector of carrier multipliers for use by the transmitter and receiver.

The second function is the transmitter shown in Figure 3.4. This function is responsible for generating the transmitted waveform by generating a random binary waveform b_i which is modulated by MFSK. The resultant waveform is multiplied by the frequency hopped carrier frequencies, $c(t)$, produced by the hop set generator.

The third function is the receiver shown in Figure 3.5. This function is where the three generated waveforms (signal, noise, and interference) are combined. The resultant waveform is then multiplied by the same carrier frequency waveform to return the signal

of interest to baseband for demodulation. This process is repeated for a range of spectrum sensing to environment change ratios. The duty cycle of spectrum sensing is fixed but the environment change is probabilistic. Basic operations such as filtering are omitted from Figure 3.5 for simplicity.

A subset of the simulated experiments will be conducted in a HIL setup using WARPLab. In this configuration, all baseband processing will be conducted using MATLAB. This processing includes data generation, symbol modulation, FH synthesis, symbol detection, REM creation and metric calculations. The transmit waveforms are uploaded to the transmit board and the resultant receive waveform is downloaded from the receive board via ethernet. All transmit data is transmitted at RF over copper with an RF combiner. The interfering waveform is generated and transmitted in the same manner as the random data bit stream but with a third radio. An overview of the hardware configuration for WARPLab is depicted in Figure 3.6.

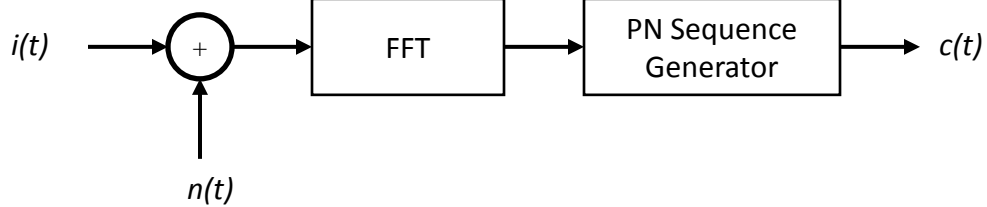


Figure 3.3: Hop set selection function model.

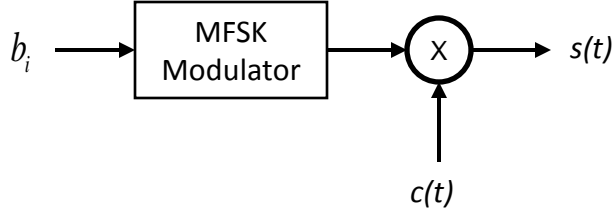


Figure 3.4: Transmitter function model.

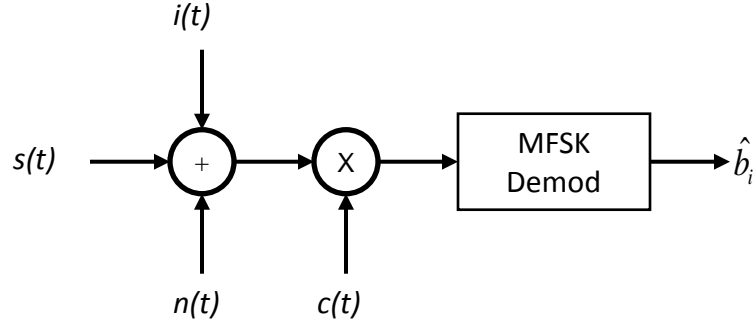


Figure 3.5: Receiver function model.

3.9 Experimental Design

The three interference profiles enumerated in Section 3.4 combine with the PN sequence refresh rate to form a full factorial design. There are 2 factors with 8 and 5 levels resulting in a total of 40 simulation experiments with an additional 8 experiments implemented in hardware. Each experiment is a Monte Carlo simulation with many independent trials (on the order of 10^5 to 10^6). The actual number of trials necessary for each data point is based on achieving a 95% confidence interval no wider than one fifth of

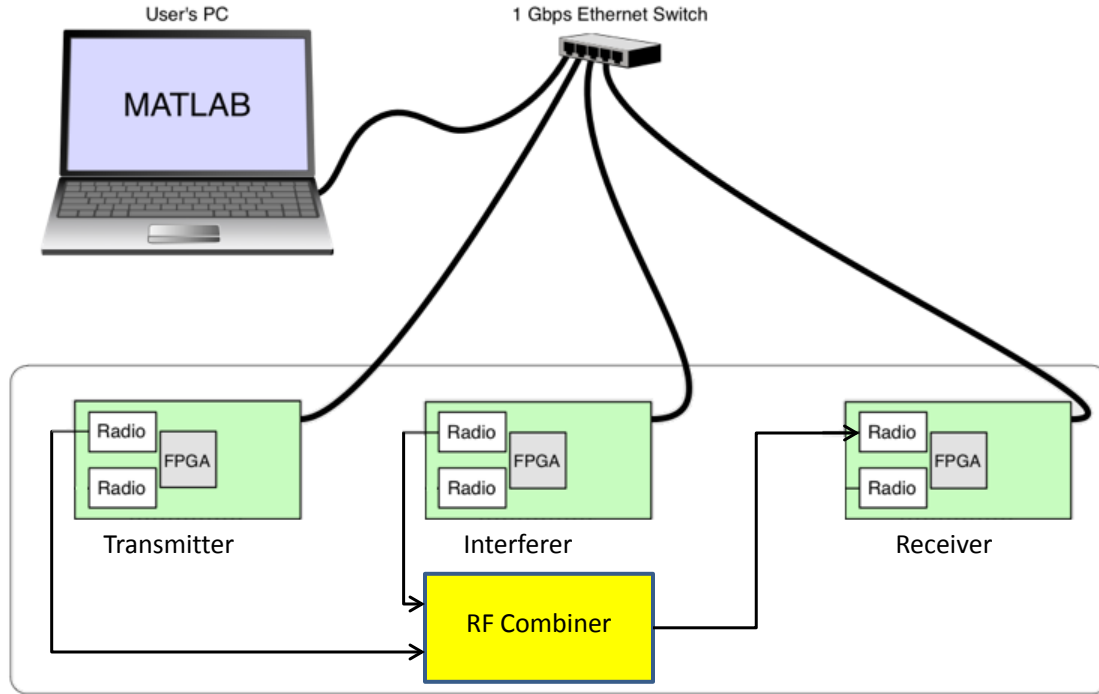


Figure 3.6: WARPLab functional diagram [16].

the sample mean. This approach provides the basis for drawing statistically supportable conclusions in the analysis.

3.10 Modem Operation

The FHSS model is intended to be implemented in hardware on the Wireless Open-Access Research Platform developed by Rice University. The characteristics of this platform drive most design choices for this model. The model implements a length 32 PN sequence that shifts the carrier frequency at a rate of one or three chip (frequency hop) per symbol. Since this particular implementation will not be used for MA communications, a simple periodic sequence is created using the `randperm(n)` function in MATLAB. This function generates a vector of positive integers 1 to n such that each integer appears exactly once.

Baseband modulation is conducted using MATLAB's built-in function `fskmod`. This function receives a vector of binary input, desired tone spacing and number of samples and provides a complex envelope for FSK modulated symbols. FSK modulation is selected for this model as it is typical of FHSS systems [10]. Tone spacing is $1/T_C$, where T_C is the chip duration. This minimum separation is required to prevent symbol aliasing in noncoherently detected FSK FH systems [31].

Each complex baseband modulated symbol is multiplied by a complex carrier determined by the PN sequence discussed above. This spreads the total system bandwidth from $W_{MFSK} = 2/T_C$ to $W_{SS} = (2 \times 32)/T_C$ at intermediate frequency (IF). Finally, the complex IF signal is modulated with a RF carrier to simulate the transmission of a real signal.

The receiver sums the received signal and AWGN. The filtered RF signal is then brought down to IF. The now complex signal is multiplied by the appropriate complex carrier to return the signal to baseband. The demodulator is a two channel correlator implementation of a noncoherent FSK demodulator. This allows for symbol estimation based on energy detection thereby mitigating potential impacts of phase error. A high level functional block diagram of the system described above is depicted in Figure 3.2.

To assess performance, the system is evaluated for BER over a desired range of E_B/N_0 dB (the ratio of average bit energy to noise spectral density). In this simulation both the transmitter and receiver operate synchronously. Relevant simulation design parameters are shown in Table 3.2.

3.11 Methodology Summary

The specific goal of this research is to determine if applying DSA to a FHSS communication system has an appreciable impact on improving BER in an environment with interference present. This objective supports the broader area of research in CR.

Table 3.2: FHSS simulation design parameters.

Parameter	Symbol	Value
Center frequency	f_C	10 MHz
Sample frequency	f_S	40 MSamp/s
Symbol rate	R_S	78.125 KSymbols/s
FSK bandwidth	W_{MFSK}	469 KHz
Number of FH channels	N_{Ch}	32
Chips per symbol	N_{CPS}	3
Spread spectrum bandwidth	W_{SS}	15 MHz

The research is conducted by introducing spectrum sensing and a more flexible sequence generation process to a more traditional FHSS implementation. Performance evaluation is conducted primarily with respect to BER with throughput also considered. The workload is selected to characterize the performance impact over a range of interference scenarios. System factors are chosen to assess the interactions between the interference scenarios and speed of adaptation. To conduct the experiment the SUT is modeled and simulated in MATLAB with simulation performance validated against theoretical BER expressions. The experimental design is full factorial with 40 experiments conducted in simulation. A subset of the simulation experiments are reproduced in a HIL setup for comparison.

IV. Results

THE following is a detailed discussion of experimental results. First, a validation of the subject model is provided. Provided the working model an assessment of DSA performance is presented for three interference profiles via simulation. Finally, the results of a HIL implementation of the modem are presented. The simulation results show that in some cases as the sensing rate increases relative to the rate of environmental change, BER does improve. As might be expected, HIL results do corroborate this observation, but the effects are much less pronounced.

4.1 Simulation Results

4.1.1 Model Validation.

To validate the MATLAB model of the experimental modem, several pilot simulations are performed. Where applicable these simulations are compared with known analytic expressions to ensure the modem is performing as desired. These pilot simulations consist of M -ary FSK without interference, a FH baseline without interference, and a FH baseline with interference. Together, these simulations demonstrate the model's suitability for obtaining reliable results in later sections.

4.1.1.1 FSK Baseline.

The first pilot simulation is of a simple MFSK modem using noncoherent detection. The model is able to support a range of bit rates as well as bits per symbol. The analytic expression for the probability of symbol error in an equally likely, noncoherently detected MFSK system is [36]

$$P_E(M) = \frac{1}{M} \exp\left(-\frac{E_s}{N_0}\right) \sum_{j=2}^M (-1)^j \binom{M}{j} \exp\left(-\frac{E_s}{jN_0}\right) \quad (4.1)$$

where M is the number of symbols in the signaling alphabet, E_s is the average energy per symbol in joules, and N_0 is the noise spectral density in watts per hertz. The relationship

between the probability of symbol error and the probability of bit error (i.e. BER) is characterized by [36]

$$\frac{P_B}{P_E} = \frac{M/2}{M-1}. \quad (4.2)$$

Simulation results are shown in Figure 4.1 for $M = \{2, 4, 8\}$ without filters. In each case, the confidence intervals⁶ of the simulated data points contain the analytic mean value.

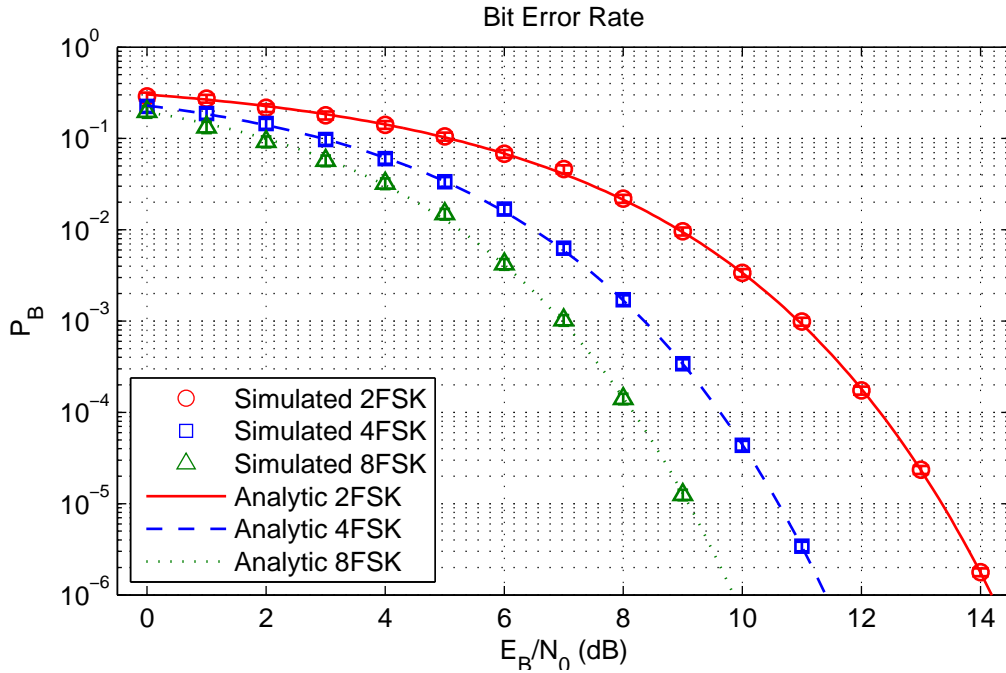


Figure 4.1: Baseline M -FSK performance (without filters).

The second pilot simulation is a repeat of the first with filters added. The filters consist of an RF front-end filter with a passband approximately equal to the total system bandwidth, W_{SS} , and a baseband filter approximately equal to the baseband bandwidth of the signal, W_{MFSK} . Simulation results for the same three cases are shown in Figure 4.2. As expected (given the method of symbol detection), the simulation slightly outperforms the analytic expression for all three cases. The performance advantage is greatest for the case

⁶In all figures, 95% confidence intervals are shown though they may be no wider than the data marker.

where $M = 2$ and is reduced as M increases. This is due to the lowest and highest frequency symbols facing a greater effect from the non-ideal corners of the filters.

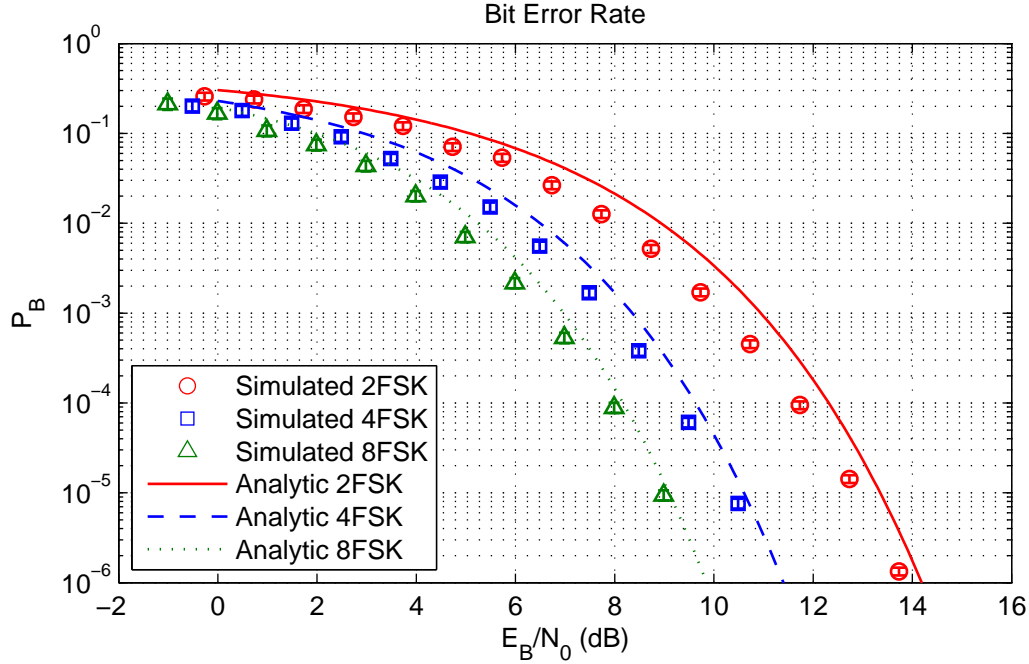


Figure 4.2: Baseline M -FSK performance (with filters).

The two pilot simulations previously described demonstrate that the MFSK model performs as expected in an AWGN channel.

4.1.1.2 FH Baseline.

Having demonstrated the functionality of the underlying modulation scheme, attention is focused on binary FSK for the remaining results. To verify the operation of the FH modem, the BER is compared to the previously simulated binary FSK results (with filters). This comparison is depicted in Figure 4.3 for a 32 channel system where $R_C = R_S$ and a 32 channel system where $R_C = 3R_S$. The consistent grouping for each of the three scenarios demonstrate that the FH modem performs similarly to the underlying non-FH

modem. The variation that is seen in the data is due to the different filter bandwidths necessary to accommodate each of the three systems.

To verify the the performance of the FH modem in the presence of interference, simulation results are compared to the analytic values determined by Equation 2.1. The interference model is a tone constrained to occupy one FH channel with sufficient energy to guarantee a bit error if the communication symbol is transmitted on the interfering channel. Figure 4.4 shows the simulated performance limit for 32, 64, and 128 FH channels along with the analytic approximation. While the modem performs symbol-by-symbol detection and the analytic expression describes chip-by-chip detection, the comparison is still useful for the case where $R_C = R_S$. These results show that as SNR increases and the interference dominates the BER, the simulated performance is closely approximated by the analytically determined values from Equation 2.1.

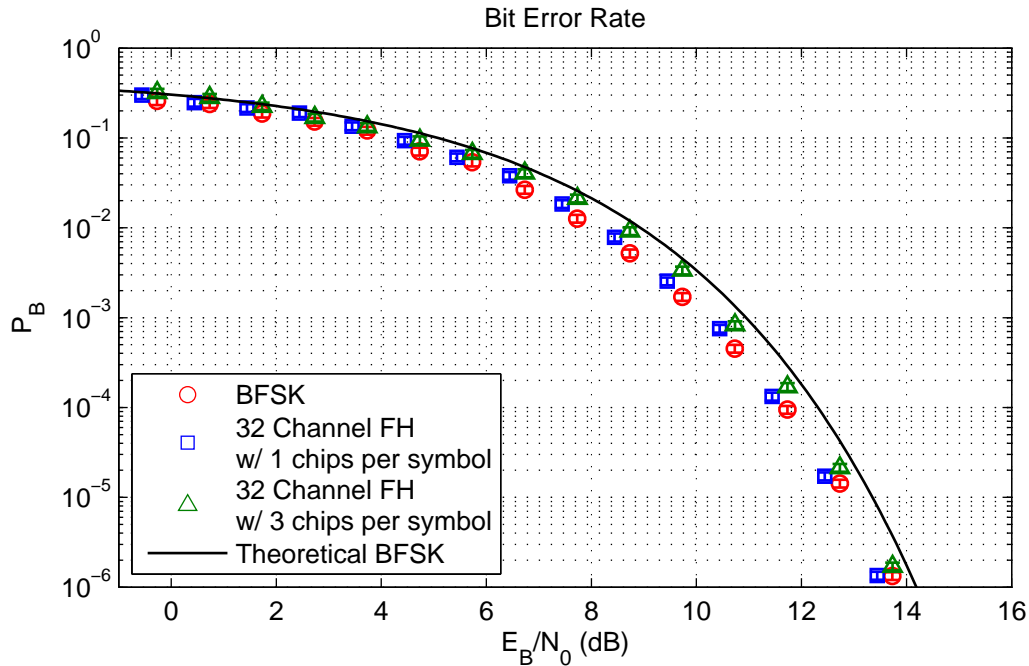


Figure 4.3: Baseline FH performance (without interference).

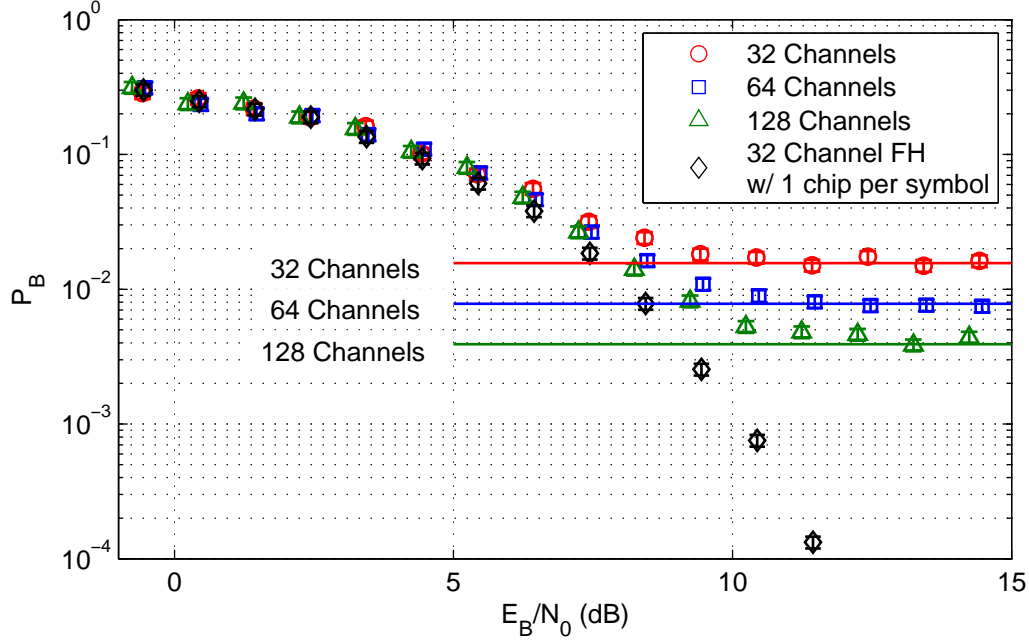


Figure 4.4: Baseline FH performance (with interference).

4.1.1.3 Spectrum Sensor.

With a validated baseline FHSS modem, spectrum sensing is added to enable the modem to modify its PN hopping sequence. The spectrum sensor is a single threshold energy detector. To demonstrate its functionality, Figure 4.5 depicts the sensor identifying four occupied channels. With this information the modem is able to attempt to avoid the interfering signals.

4.1.2 DSA Performance.

With model functionality validated, the performance of the DSA modem can be compared to the baseline performance of the FH modem without any interference. The results below follow the pattern of first identifying a fixed value⁷ of $E_B/N_0 \approx 12dB$ and varying the ISR to determine the interference power required to degrade performance by one order of magnitude. Given this interferer power, BER curves as a function of E_B/N_0

⁷The observed baseline value of BER is 1.7×10^{-4} at $E_B/N_0 = 11.73$ dB.

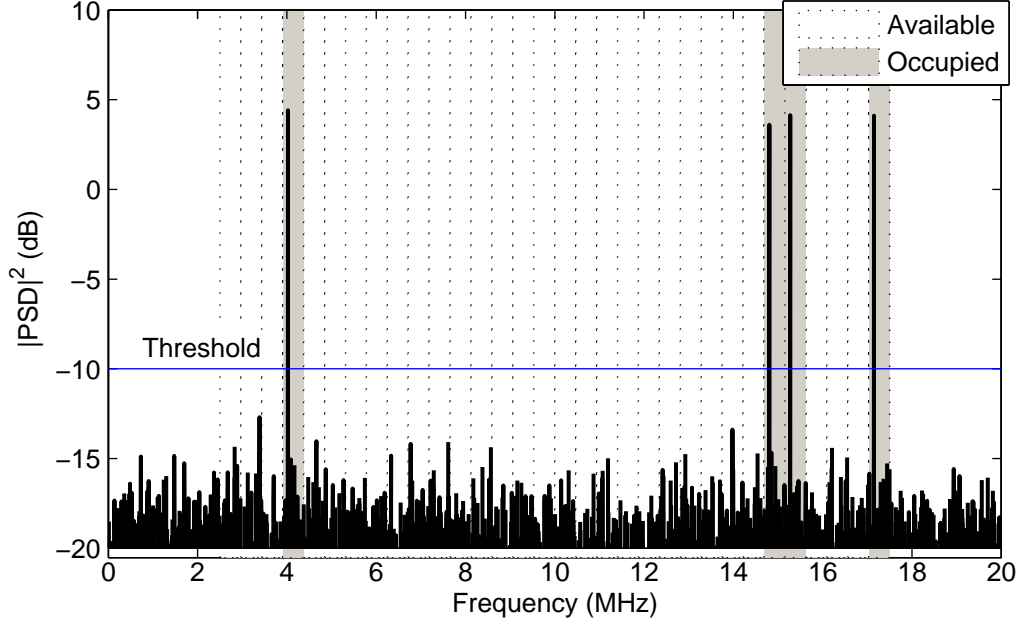


Figure 4.5: Demonstration of spectrum sensor identifying four interfering tones.

are compared against baseline performance. Finally, the spectrum sensor is enabled to observe performance as the rate of environment change is varied in relation to the spectrum sensing rate.

4.1.2.1 *Single Tone Interference.*

The most simplistic test case is that of the single tone interferer. In this scenario, a single narrowband tone will occupy the lower symbol frequency of a single channel at any given time. By constraining the frequency of the interfering tone in this way, the results represent a worst-case-scenario as the tone is located where it will have the maximum disruptive affect.

To determine the interference power required to degrade performance in the non-adaptive modem by one order of magnitude, performance is simulated over a range of ISR given a fixed E_B/N_0 . The results of this simulation are shown in Figure 4.6. The observed ISR resulting in the desired affect is approximately 4 dB.

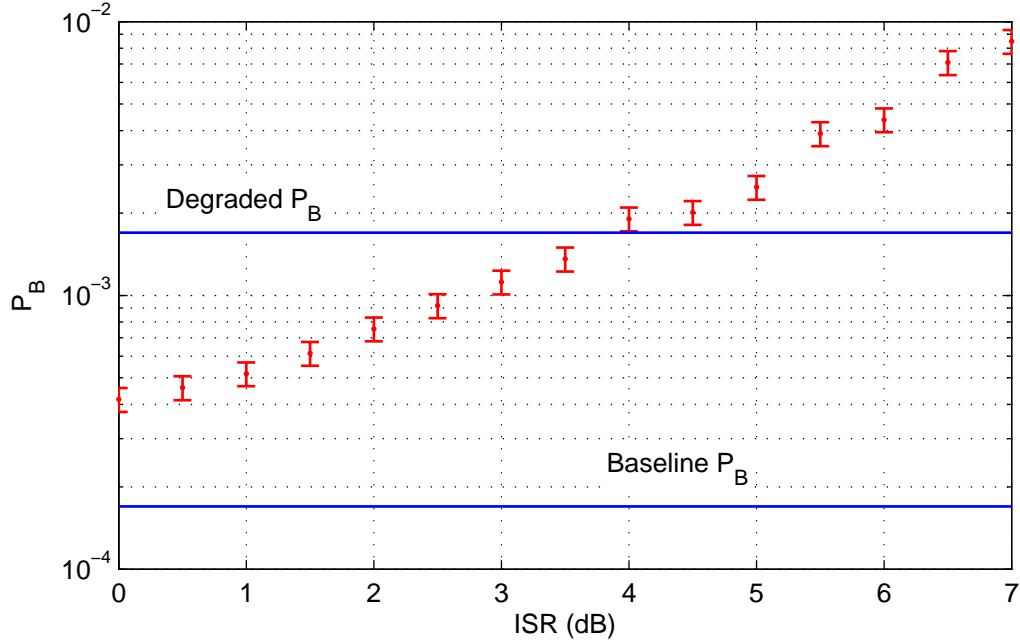


Figure 4.6: Non-adaptive BER performance as a function of ISR with one interfering tone present.

Given the fixed value of $\text{ISR} = 4 \text{ dB}$, the performance of the receiver is simulated again in Figure 4.7 over a range of E_B/N_0 for comparison with the baseline performance without interference. The results demonstrate, in a more traditional presentation of BER, the desired degradation of performance at $E_B/N_0 \approx 12 \text{ dB}$. The annotated baseline and degraded P_B (BER) serve as the anticipated lower and upper bounds of the DSA performance.

For the fixed values of E_B/N_0 and ISR determined previously, the simulation is run again with the DSA mechanisms enabled. For these simulations, the sensing interval (or rate) is fixed. The sensing duration is equivalent in time to the transmission of 32 symbols. The duty cycle consists of sensing (and adapting the PN sequence) followed by the transmission of 3200 symbols. This is repeated through the duration of the simulation. The rate of environment change is adjusted in relation to the rate of spectrum sensing.

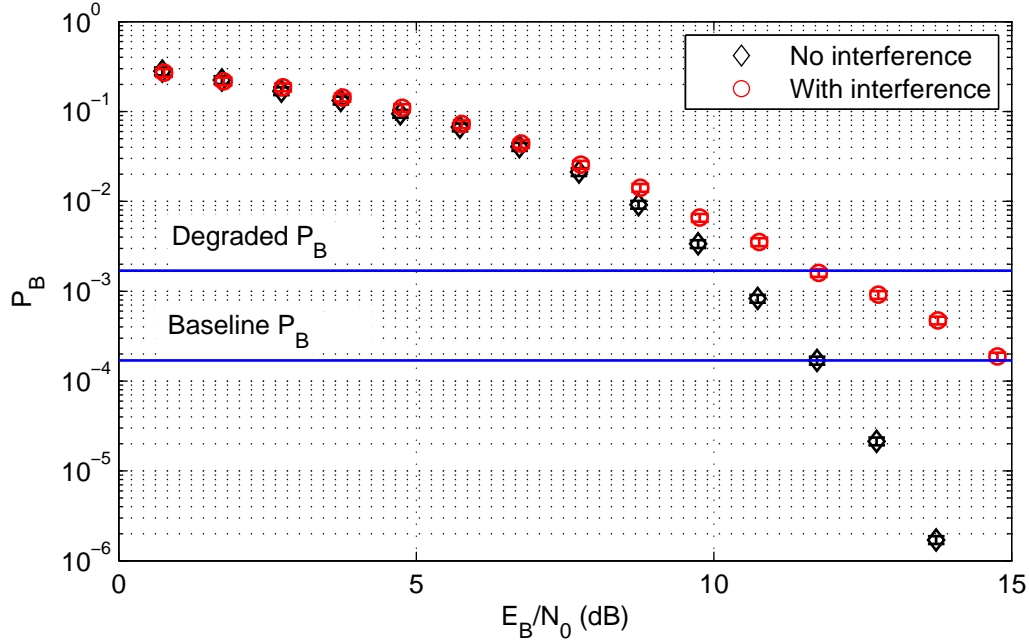


Figure 4.7: Non-adaptive BER performance as a function of E_B/N_0 with one interfering tone present.

Figure 4.8 depicts the BER performance of the receiver as the rate of spectrum sensing is increased in relation to the rate of environment change. Alternatively, the rate of environment change is decreasing from left to right. These results indicate that the BER can be measurably reduced by adapting the PN sequence at least 0.5 times as frequently as the environment is changing given the parameters selected. By sensing the spectrum 27 times as frequently as the environment is changing yields a BER that is approximately (and statistically) the same as the baseline performance. The practicality of achieving these ratios of sensing to environment change is highly application and environment dependent.

While the addition of spectrum sensing and communication waveform adaption is shown to decrease the BER, the overall throughput of the system (in bits per second) is decreased in this scenario. Figure 4.9 compares the system throughput without DSA

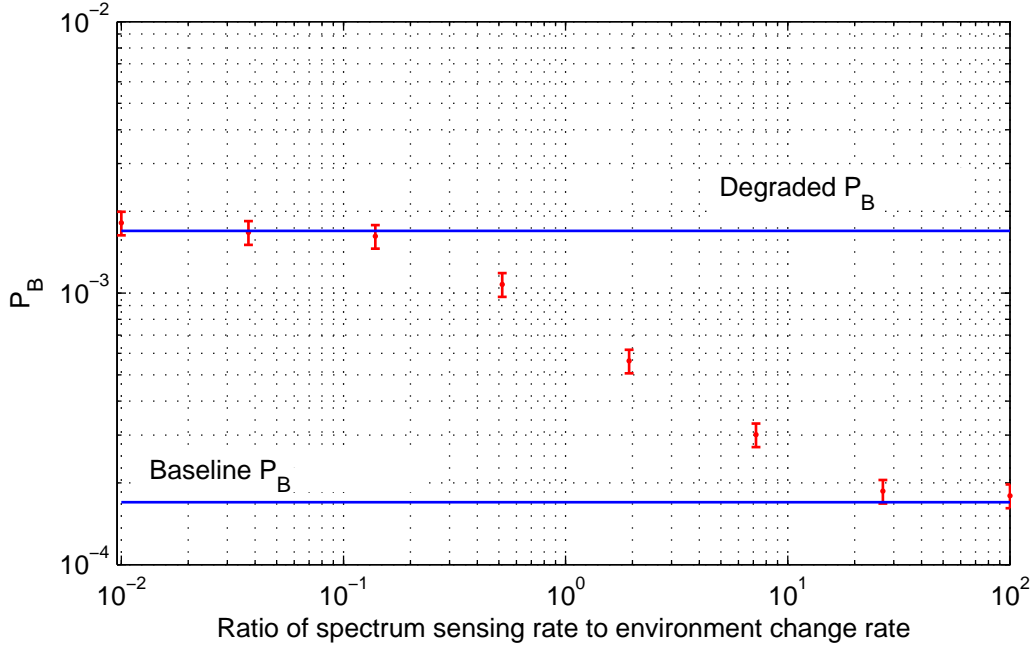


Figure 4.8: Adaptive BER performance as the spectrum sensing rate increases relative to the environment change rate with one tone interferer.

enabled to the throughput with DSA enabled. The results show that total throughput is reduced, albeit minimally. The data also demonstrate that, as expected, for cases when DSA is enabled the throughput of the system increases as spectrum sensing becomes more frequent in relation to the changing environment.

It is important to note that Figure 4.9 represents a fixed spectrum sensing rate (for all data points other than “non-DSA”). This is limiting in that the data do not represent the relationship between throughput and the spectrum sensing rate. This relationship can however be approximated. Without any interference present, the observed throughput, R'_D , approaches the system data rate⁸, R_D , providing an upper bound on performance without any spectrum sensing. When spectrum sensing is enabled, as the ratio of sensing to environment change increases and BER approaches zero (again, with no interference

⁸In binary signaling the data rate is equal to the symbol rate (i.e. $R_D = R_S$)

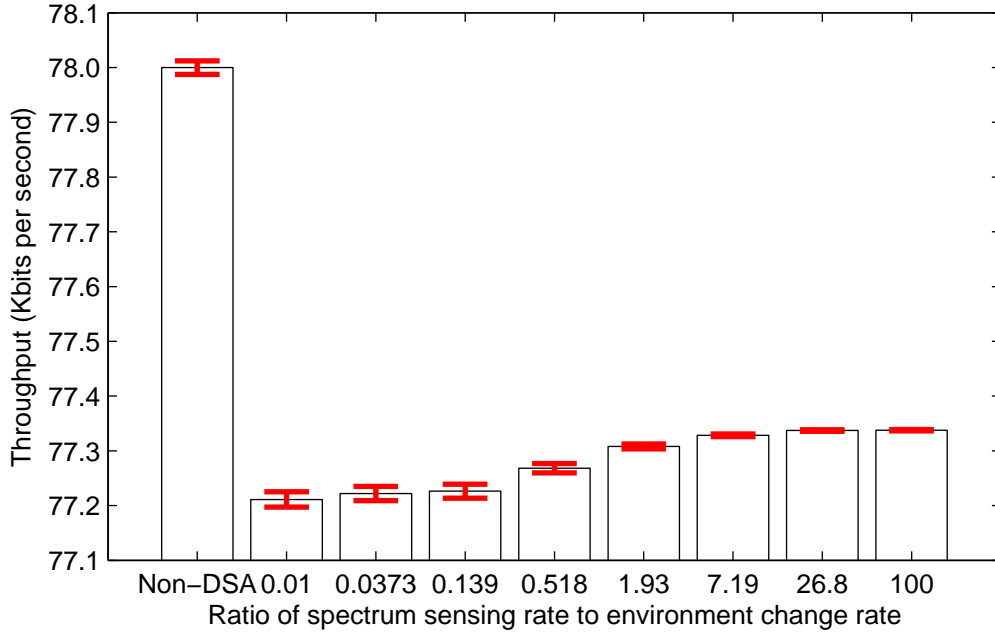


Figure 4.9: Throughput of FHSS system for multiple ratios of spectrum sensing rate to environment change rate with one tone interferer present.

present), throughput approaches

$$R_D \times \frac{\text{time spent sensing}}{\text{time spent transmitting}}.$$

This implies that in circumstances where the environment is changing slowly and the impact of interference to a non-adaptive modem is much more significant, enabling DSA could, in fact, improve throughput in addition to BER.

4.1.2.2 Multi-tone Interference.

To increase the complexity of the interference, additional tones are added to the environment. In this model, the same constraints apply to each tone as in the last section. That is, each interfering tone occupies only one FH channel at any given time. Furthermore, the interfering tones occupy the same frequency as one of the transmitted symbols to present a worst-case outcome for the individual trial. Interfering tone frequencies are assigned randomly such that there are always exactly the number of tones

desired. For example, given a two tone interference model, the probability of both tones being assigned to the same FH channel is zero. The performance of the receiver given this interference model is examined for 2, 4, and 8 tones.

The process of determining the ISR necessary to degrade BER performance by one order of magnitude is repeated for each tone count as described in the previous section. The outcomes of this process are shown in Figure 4.10. There is little statistical distinction between the three experiments; however, it is expected that as the number of tones increases and the power is split between those tones, the average power required to result in a bit error increases. For this reason, the value of ISR at which the performance intersects (within the 95% confidence intervals) the desired BER is evaluated independently for each of the three scenarios. The resulting values of ISR are shown in Table 4.1.

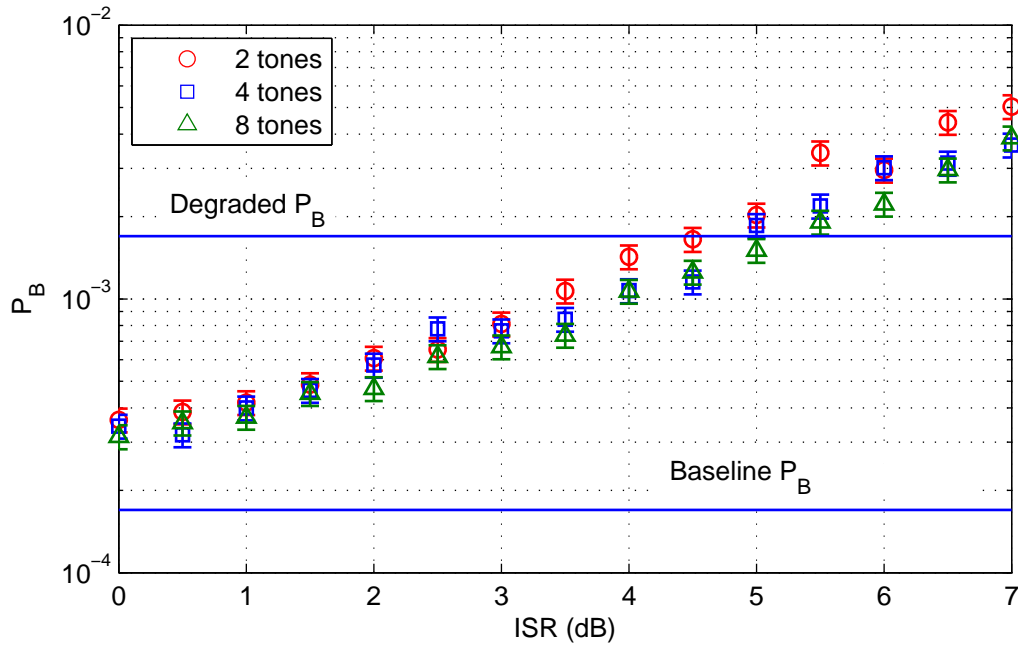


Figure 4.10: Non-adaptive BER performance as a function of ISR with multiple interfering tones present.

Table 4.1: ISR required to increase BER by one order of magnitude over baseline performance of 1.7×10^{-4} .

Number of tones	ISR (dB)	Observed P_B
1	4	1.90×10^{-3}
2	4.5	1.65×10^{-3}
4	5	1.85×10^{-3}
8	5.5	1.91×10^{-3}

With the desired ISR for each scenario obtained, the simulations are repeated over a range of E_B/N_0 . The results are shown in Figure 4.11 for comparison with the baseline performance. Again, there is little statistical difference between the three scenarios for the range of E_B/N_0 simulated. Since the simulated values of P_B for each scenario contained the desired reduction in performance within the confidence intervals, only one line is drawn to depict the degraded P_B .

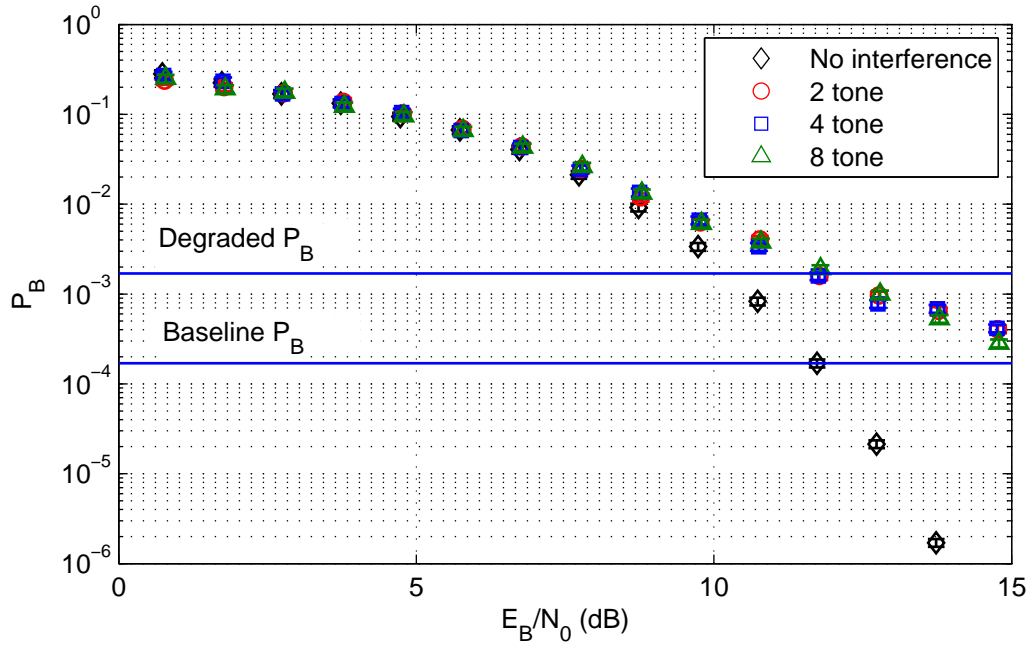


Figure 4.11: Non-adaptive BER performance as a function of E_B/N_0 with multiple interfering tones present.

The process of evaluating modem performance with DSA enabled is repeated for each multi-tone scenario as described in the previous section. Each scenario is evaluated at a fixed E_B/N_0 and fixed ISR over a range of sensing to environment change ratios. The results, shown in Figure 4.12, are somewhat surprising in that there is very little statistical difference between the three scenarios. It might be expected that as the portion of FH channels that are interfered with increases, the capability of the DSA modem to avoid those channels would be reduced. This, however, is not conclusively supported by the results observed. The results indicate that the modem is similarly robust provided some portion of the channels remain available for use.

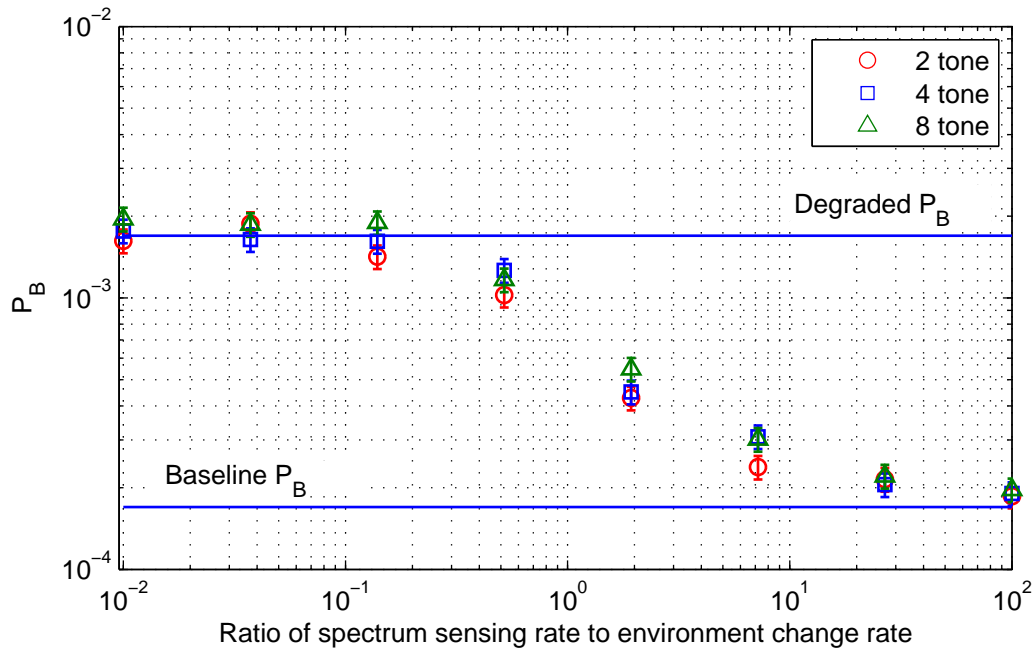


Figure 4.12: Adaptive BER performance as the spectrum sensing rate increases relative to the environment change rate with multiple tone interferers.

As with the single tone interferer, the modem is effective in reducing the BER provided a fast enough sensing cycle in relation to the rate of change in the surrounding environment. Again, as with the single tone model, the implementation of DSA does

reduce the overall throughput of the system. The throughput for each of the three scenarios is compared with the non-DSA throughput in Fig 4.13.

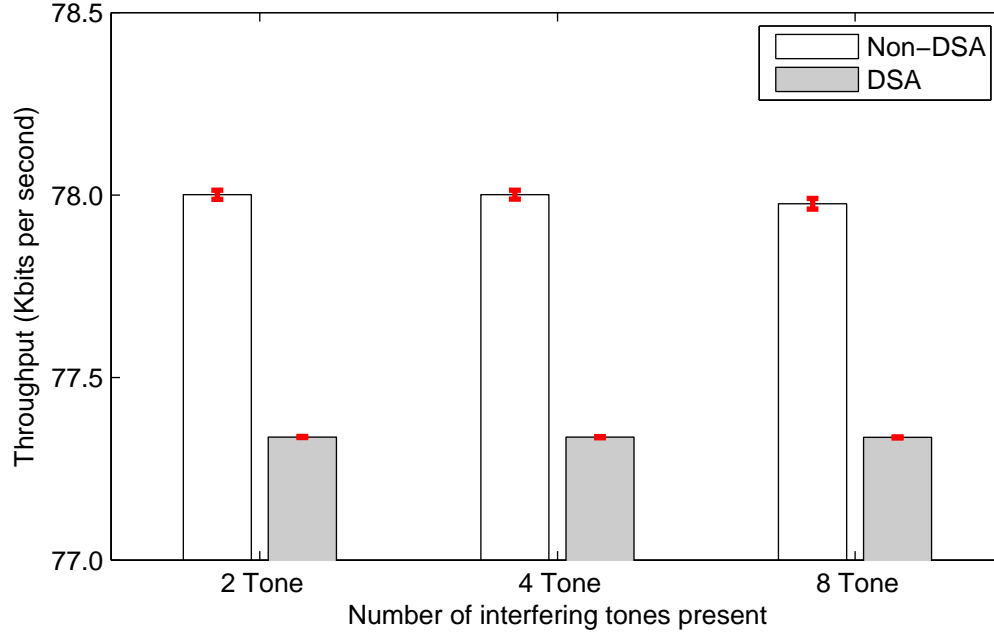


Figure 4.13: Throughput of FHSS system for multiple ratios of spectrum sensing rate to environment change rate for 2, 4, and 8 tone interferers present.

4.1.2.3 Wideband Interference.

As an alternative to the tone interference models, wideband interference is considered. Here, wideband refers to a signal whose spectrum spans the entirety of the experimental modems RF front end. This interference model is implemented using an OFDM waveform which provides a relatively uniform PSD over the system bandwidth. The OFDM waveform is generated by modulating 4-ary phase-shift keying (PSK) communication symbols on 128 sub-carriers with a circular prefix of length 32. The frequency encoded waveform is oversampled by a factor of three to achieve a sufficient bandwidth to span the entirety of the DSA modem front end filter.

As in the tone interference models, the first step is to identify the average interference power required to degrade the non-DSA receiver BER performance by one order of magnitude. To do this, for the same fixed value of E_B/N_0 determined previously, the interfering waveform is transmitted continuously for an increasing range of ISR. The result of this experiment is shown in Figure 4.14. The point at which the interference reaches the desired threshold is $\text{ISR} = 15 \text{ dB}$. If this value of ISR seems high, recall that the bandwidth of the OFDM waveform exceeds the bandwidth of the filter. A significant portion of the interfering waveform power has little to no influence over the receiver performance. Additionally, while the OFDM waveform is a structured signal it is considerably more “noise-like.”

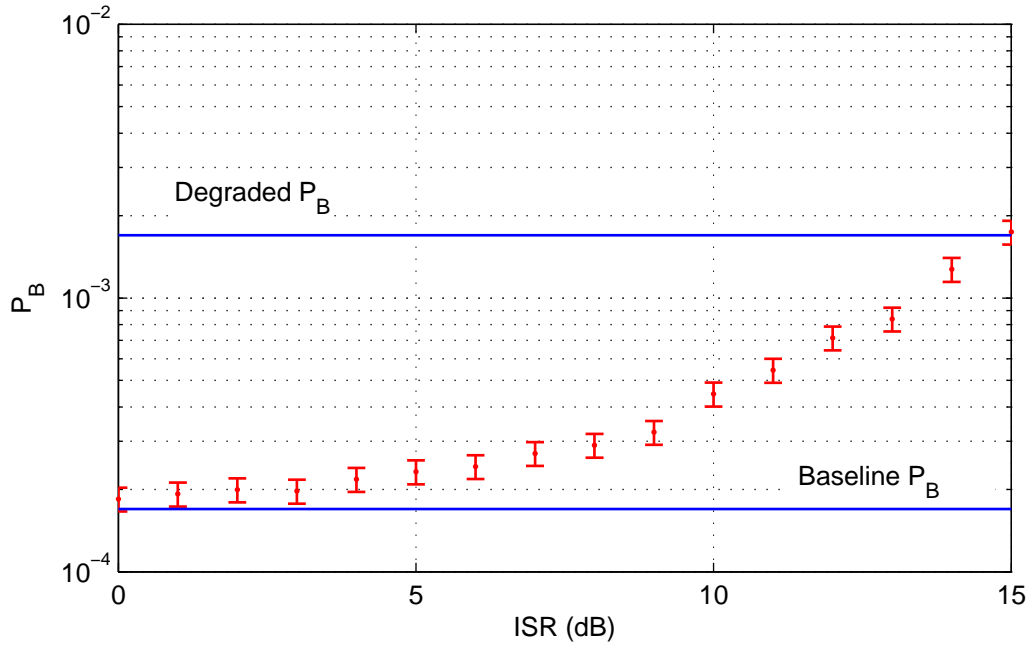


Figure 4.14: Non-adaptive BER performance as a function of ISR with OFDM interference present.

Given the required ISR, the BER performance is again simulated over a range of E_B/N_0 for comparison with the baseline performance. The result of the simulation is shown in Figure 4.15.

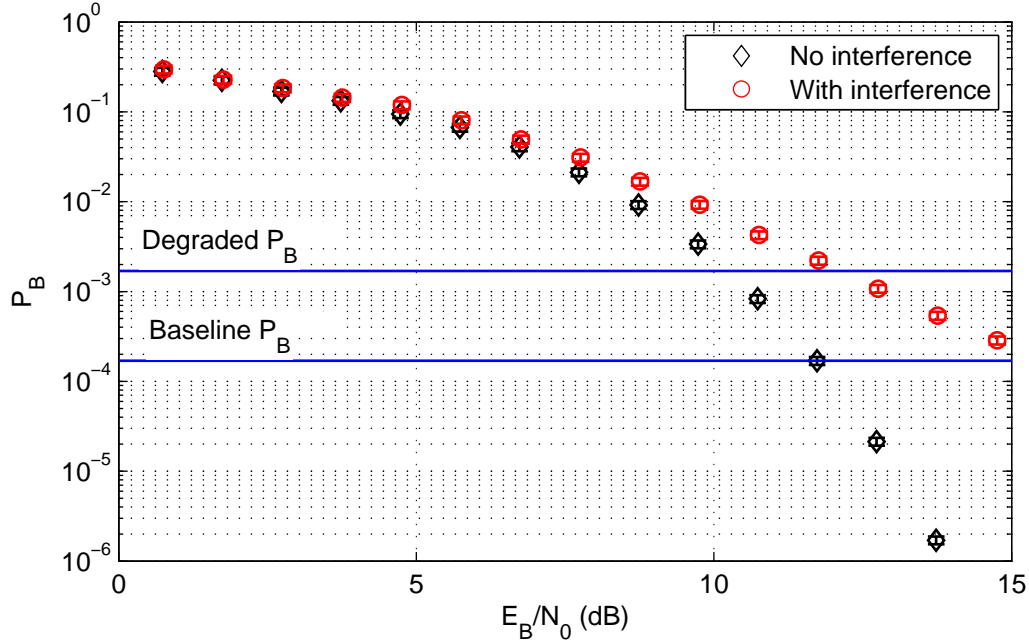


Figure 4.15: Non-adaptive BER performance as a function of E_B/N_0 with OFDM interference present.

In this scenario, the limitation of energy detection as the method of spectrum sensing becomes clear. By leaving the sensing threshold at 10 dB above the ambient mean, as in the tone interference experiments, the PN sequence generator will rarely (if ever) drop a FH channel due to interference. Even with the sensitivity of the spectrum sensor reduced to three dB above ambient mean the interfering spectrum is changing on an OFDM symbol-by-OFDM symbol basis. In this case, the PSD is changing very rapidly as there are more than 32 OFDM symbols (each with its own frequency domain encoding) in the duration of a single spectrum scan. This rate of environment change is not practical for the spectrum sensor to attempt to out pace.

Rather than attempt to characterize the DSA performance for a range of spectrum sensing to environment change ratios as in the previous two sections, performance here is characterized as a function of the portion of time that the interferer is transmitting. This is a break from the experimental method from Chapter 3; however, it provides a more relevant comparison between the adaptive and non-adaptive configurations. To do this, instead of transmitting a constant stream of OFDM symbols, the interfering waveform is modelled after the packetized bursting behaviour characteristic of 802.11 networks implemented using OFDM. BER is assessed as a function of the percentage of time the interferer is transmitting for both the DSA and non-DSA configurations. The results, shown in Figure 4.16, show that the BER performance of the DSA modem is statistically the same as the non-DSA modem.

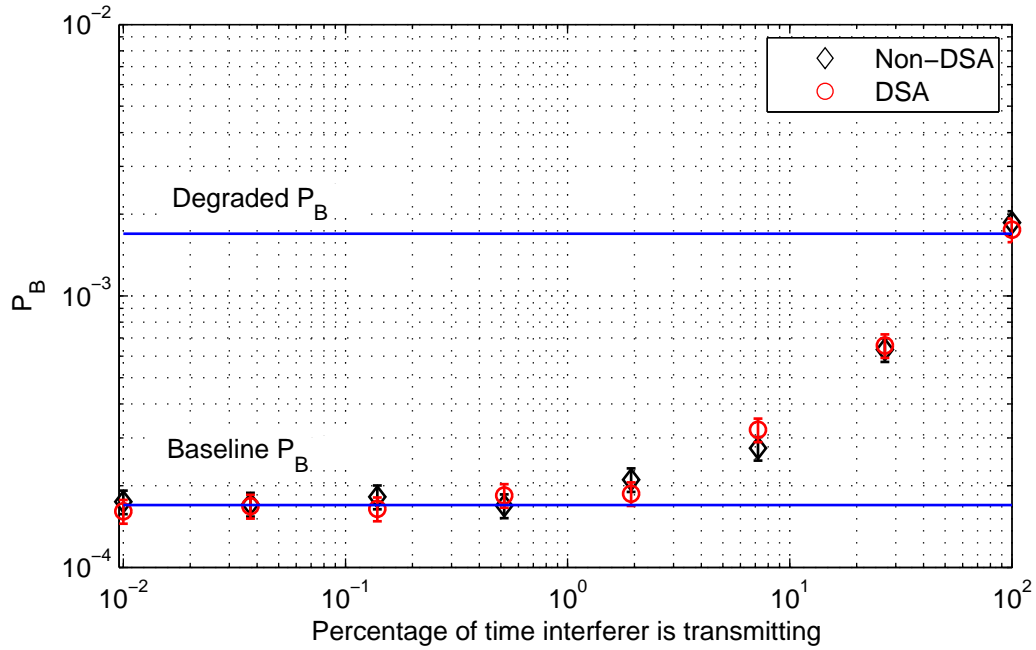


Figure 4.16: Adaptive BER performance as the spectrum sensing rate increases relative to the environment change rate with OFDM interference.

In this scenario, not only does the implementation of DSA offer no improvement to BER, it also reduces overall throughput by approximately 1%, as this is the penalty to maximum theoretical throughput for sensing at this rate (i.e. 1 sensing cycle equal to 32 symbol durations per 3200 symbols transmitted). The throughput of the non-DSA modem is compared to the DSA modem as the rate of interferer transmission increases in Figure 4.17.

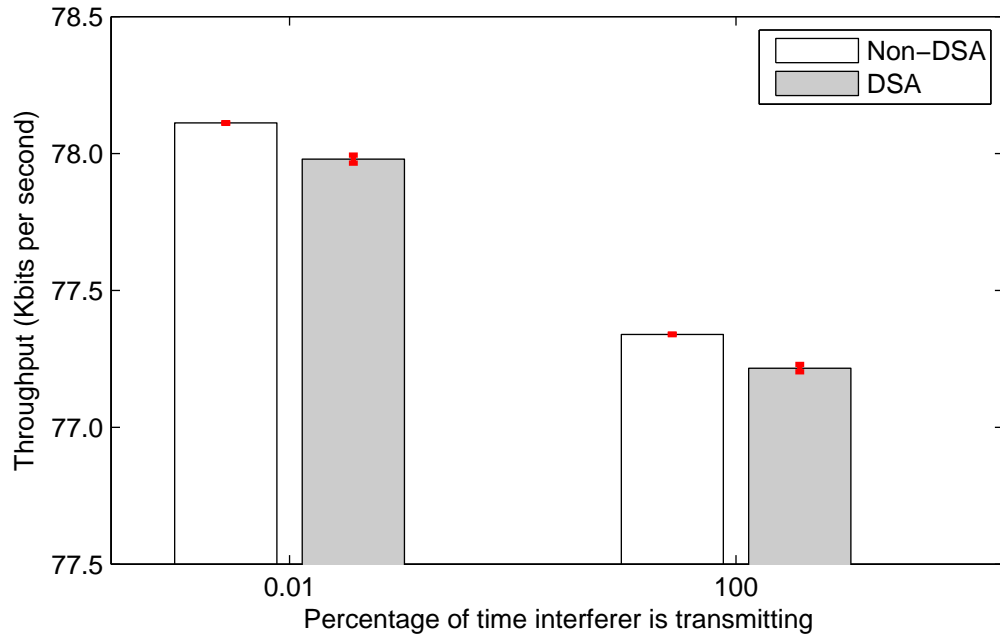


Figure 4.17: Throughput of FHSS system for multiple ratios of spectrum sensing rate to environment change rate with one tone interferer present.

4.2 Hardware-in-the-Loop Results

To corroborate simulation results as well as provide a limited hardware demonstration of the experimental DSA modem, the MATLAB model is ported to WARPLab 7. Porting the model consisted of adding function calls where appropriate to interface with the WARP radios and disabling any RF processing in MATLAB as all

passband signal processing is executed by the WARP board itself. WARPLab 7 provides a HIL development and testing framework to reduce the necessary hardware and embedded development necessary to implement a physical prototype.

4.2.1 Validation and Baseline Performance.

As with the MATLAB model, the modem is first operated as a single channel FSK modem (without FH) to compare actual performance with theoretical performance. Right away, the constraints of using real devices transmitting over real transmission media become apparent. Figure 4.18 shows the performance of the underlying binary FSK modem compared with theory. At approximately 12.5 dB, factors other than AWGN begin to dominate the induced BER. By 13.5 dB the HIL implementation is committing 10 times as many bit errors as the simulation.

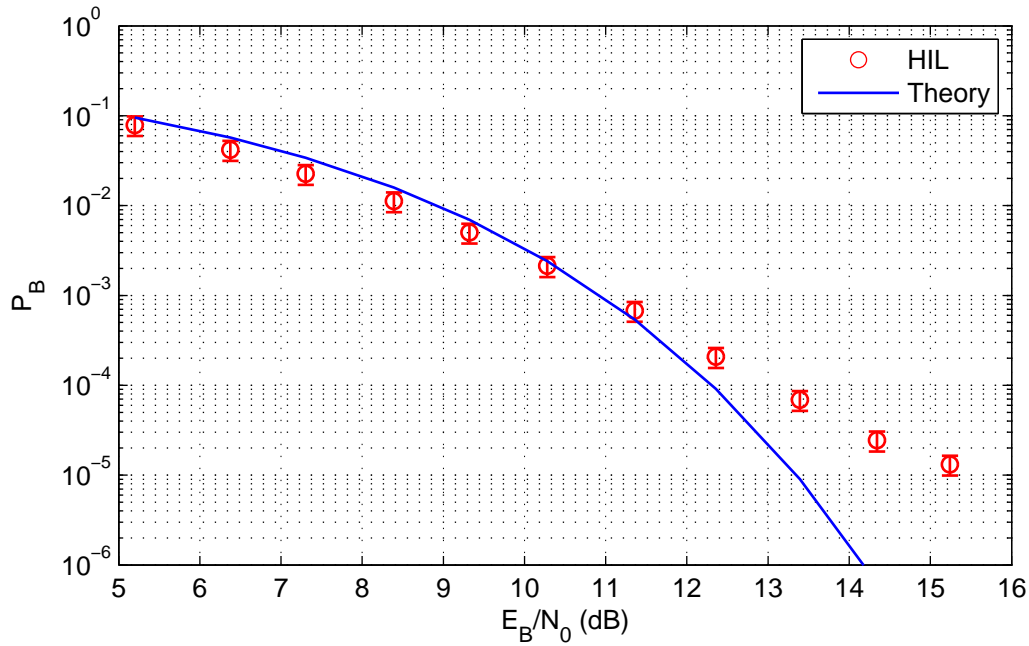


Figure 4.18: Baseline HIL FSK performance.

The impact of the limitations of physical reality become much more pronounced as the number of FH channels and the number of chips per symbol increase. For this reason,

the HIL model is configured to hop over just four channels with only one chip per symbol. The baseline results for this experiment are shown in Figure 4.19. From these results, the baseline value of E_B/N_0 to anchor the following results is 27.4 dB. The observed corresponding value of P_B is 2.0×10^{-4} .

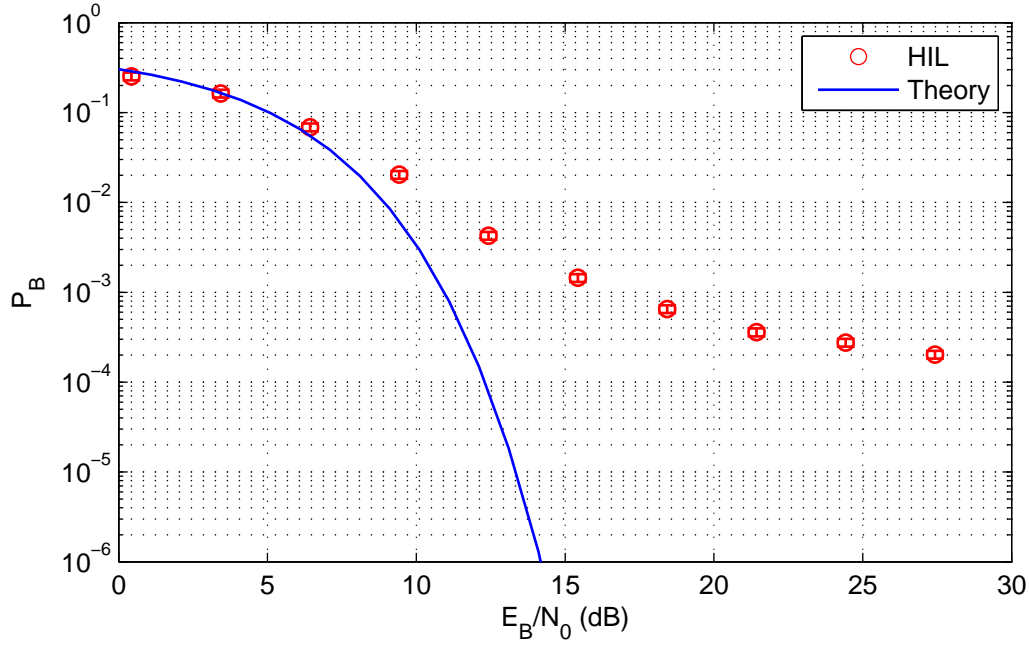


Figure 4.19: Baseline HIL FH performance.

4.2.2 DSA Performance.

For the HIL configuration, the single tone interference model is considered again. This interference model operates as described above with the reduced number of FH channels to occupy. As with the simulated results, the HIL configuration is tested with a fixed E_B/N_0 over a range of ISR to determine the point at which BER performance is degraded by one order of magnitude. The results are shown in Figure 4.20. At $\text{ISR} = -11.5$ dB the observed value of P_B is 1.82×10^{-3} . The required ISR is considerably

less than was necessary in simulation largely due to the substantial reduction in available FH channels as well as the loss of frequency diversity.

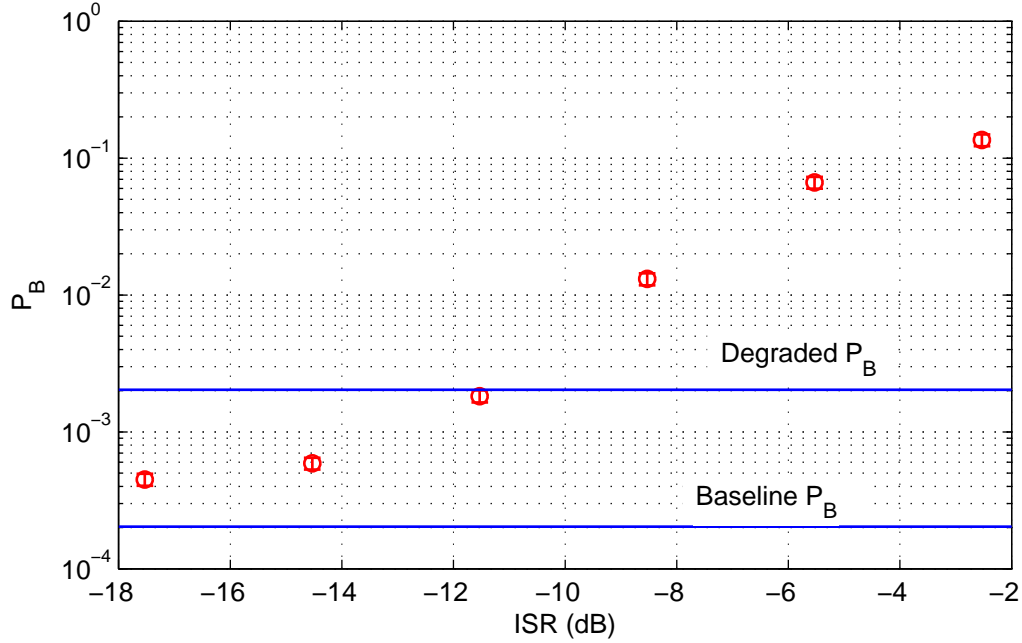


Figure 4.20: Non-adaptive HIL BER performance as a function of ISR with one interfering tone present.

Using the fixed value of ISR obtained from the previous step, the HIL configuration is tested over a range of E_B/N_0 to compare with baseline performance. These results are shown in Figure 4.21.

Finally, given the fixed values of E_B/N_0 and ISR determined previously, the modem BER performance is tested over a range spectrum sensing to environment change ratios with DSA enabled. Figure 4.22 shows that while the DSA modem is able to reduce the BER, it does not reach the anticipated lower bound (the expected value when no interference is present). This is due to reduced accuracy in the spectrum sensing process itself. The apparent increase in BER for the final data point is not unusual as it is typical to

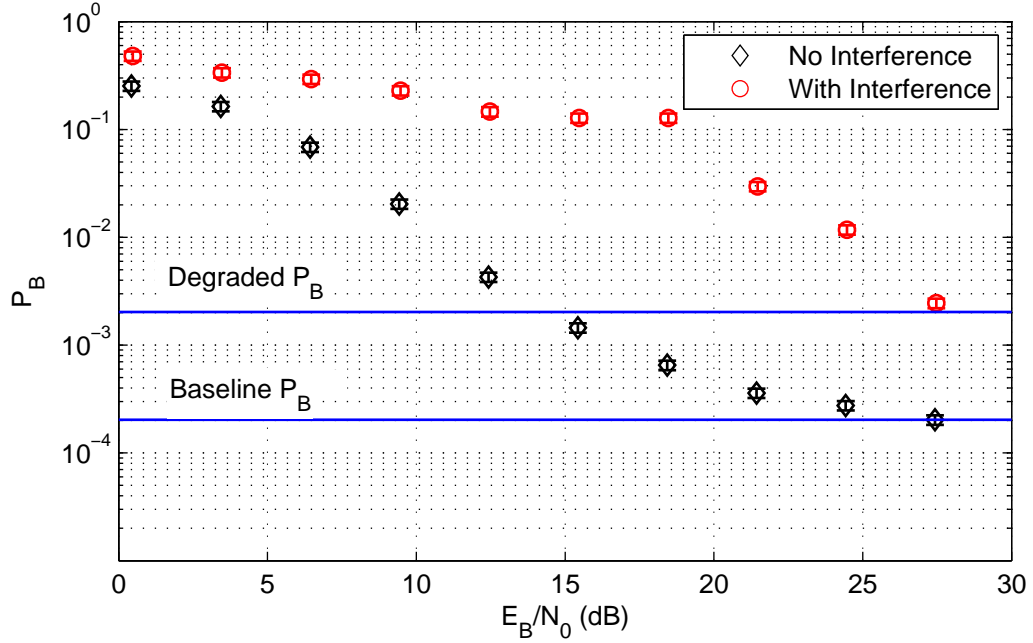


Figure 4.21: Non-adaptive HIL BER performance as a function of E_B/N_0 with one interfering tone present.

observe values that vary to the extent of their confidence intervals. This is particularly evident when a boundary is approached.

Figure 4.23 depicts the throughput of the non-DSA configuration to the DSA configuration for the HIL experiment. As with the single tone simulation, the rate of spectrum sensing causes an overall decline in the throughput of the system. Generally, as the rate of sensing increases relative to the environment change, the throughput does improve. Again, the ripples in the trend are not alarming as they are within the statistical confidence intervals given the number of trials.

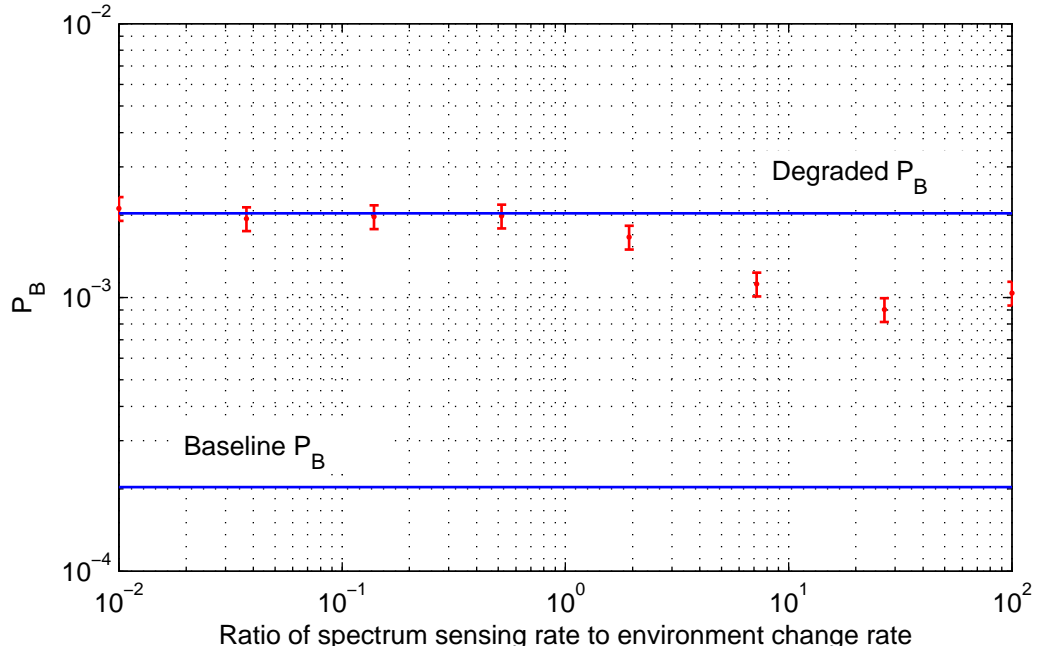


Figure 4.22: Adaptive HIL BER performance as the spectrum sensing rate increases relative to the environment change rate with one tone interferer.

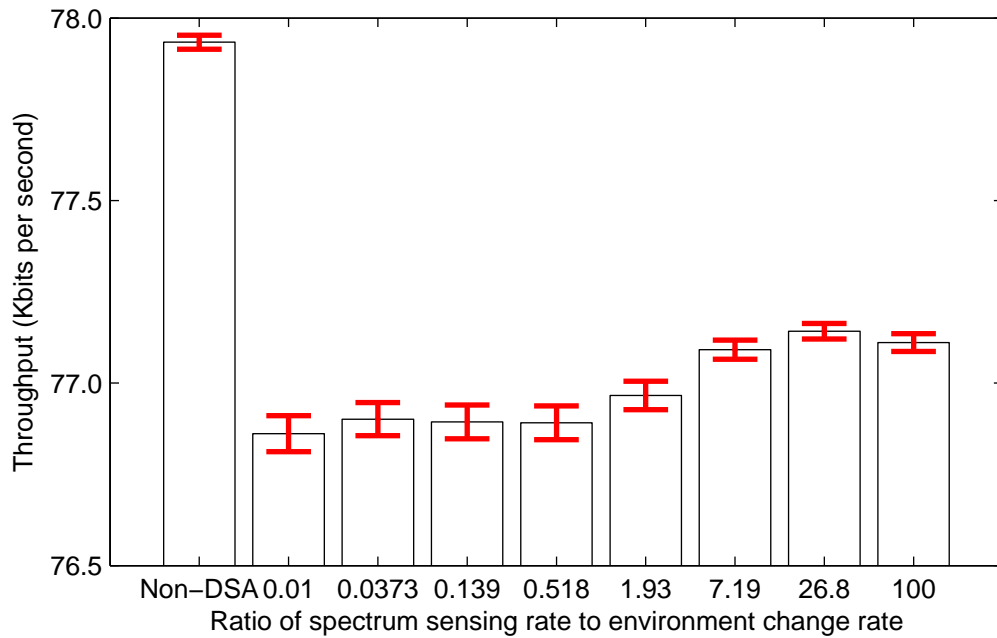


Figure 4.23: Throughput of FHSS system for multiple ratios of spectrum sensing rate to environment change rate with one tone interferer present.

V. Conclusions

THIS chapter summarizes research in the design and evaluation of an experimental fast FH modem that leverages DSA techniques to avoid interference and improve performance. Implications of the results in Chapter 4 are discussed. Finally, recommendations for future research based on the findings of this effort are presented.

5.1 Summary

The purpose of this research was to investigate the efficacy of implementing DSA in a traditional non-adaptive modem to improve the reliability of communication. To accomplish this an analysis of existing spread spectrum and DSA technologies is conducted. These technologies are evaluated in the context of the AFIT CR model.

The implementation of fast FH is selected for its robustness against interference as well as the relative ease with which the transmitted spectrum can be modified. Given the large instantaneous narrowband spectra of FH transmitters, opportunistic access (spectrum overlay) is chosen as the method of DSA. Energy detection is used to conduct spectrum sensing and enable opportunistic access. Energy detection is relatively simple to implement and as this prototype model is primarily concerned with avoiding interference (as opposed to avoiding interfering with other systems), it is also sufficient for identifying unavailable spectrum and creating a REM. In accordance with the ongoing body of CR research at AFIT, the model is designed for portability to and demonstration on the WARP version 2.

To evaluate the performance of the DSA modem, an analysis is conducted for a control transmitter/receiver pair that does not implement DSA as well as the experimental pair with DSA enabled. These models are implemented in simulation via MATLAB and

in a HIL setup using MATLAB and WARPlab. Comparisons are made based primarily on BER and throughput.

Results demonstrate that the method of avoidance implemented is effective in reducing the BER in an environment where the spectrum is partially obstructed by interfering tones. With a sufficiently high spectrum sensing rate relative to the rate the environment is changing, BER can be reduced to approximately that of the case where no interference is present. Whether the rate is achievable in a more practical application is dependent on hardware resource capabilities as well as the nature of the environment itself. Given the prototype configuration for the experiments conducted, this improvement did result in a lower observed throughput. This is brought about because the improvement in successfully transmitted bits per second (on the order of 10^{-3}) is insufficient to overcome the lost transmission opportunities (on the order of 10^{-2}).

When the spectrum is completely obstructed by a wideband interferer, as with the representative OFDM waveform, the results are considerably less favorable. The spectrum of the OFDM waveform changes many times during the duration of a single spectrum sensing (not including communication time). The result over the spectrum sensing duration is a PSD that looks very much like noise. The result is that there is no statistical difference between BER performance of the non-DSA and DSA modems. The system throughput is decreased in the DSA system due to the lost transmission opportunity caused by pausing to sense the spectrum.

Due to the constraints of WARPLab and WARP, some modifications to system parameters were required for the HIL configuration. Most notably, the number of available FH channels was reduced from 32 to 4 and the number of chips per symbol was reduced from 3 to 1. The results demonstrated a similar trend in the single tone test case; however, the results were much less pronounced. Rather than reducing BER by an order

of magnitude and reaching the baseline performance without interference, the modem was only effective to reduce the BER by approximately one half.

In no test cases did the BER increase. In some cases the BER performance improved to the point of effectively nullifying the interfering source. While throughput was decreased in all scenarios, it is likely that the bit rate could be increased given different environmental conditions and a variable sensing rate. This research has been successful by accomplishing the following specific tasks:

1. Demonstration of applying opportunistic access in a FH modem with hardware;
2. Demonstration of reducing BER in a system implementing opportunistic access; and
3. Identifying suitable and unsuitable environmental characteristics in which the modem may be performant.

Hypothesis 1 is confirmed for partial band interference. Each of the tone interference models yielded the expected improvement in BER. In the presence of wideband interference, results show the hypothesis to not be true. Hypothesis 2 is not shown to be false given the data collected. In all interference models, the adaptive modem performed at least as well as the non-adaptive modem; however, there is not sufficient data to support the assertion that BER cannot be made worse.

5.2 Future Work

There are several opportunities available to extend this body of research. This section discusses some of those opportunities for future research.

The prototype developed to conduct this research was developed primarily as a simulation with particular consideration given to implementation using WARP. The modem was tested as a HIL experiment; however, WARP implementation has limitations. Given the successful demonstration of the modem using WARPLab, a more robust embedded implementation using the WARP's FPGA and microcontroller is justified.

This research was concerned primarily with reducing BER and some treatment was given to throughput. A more thorough examination of factors that impact throughput could provide insight that would yield more efficient use of available spectrum. Additionally, it would be beneficial to examine the impact that the design presented would have on other users in the same spectrum.

A very significant aspect of communicating not addressed here is the concept of rendezvous. The gains in BER performance and throughput mean nothing if two or more radios can not synchronize their PN sequence phase. While the synchronization of FH phase has been well explored, there is little research in rendezvous and maintaining synchronization when the sequence itself is changing over time. This is particularly true in fast FH. There is ongoing research at AFIT to address this problem; however, integration with an embedded implementation of the prototype modem presented here would provide a robust demonstration of the feasibility of the design.

Appendix: WARPLab Function Library

- `intgen.m` - This function is able to provide multiple types of randomly generated interfering waveforms. Current interference models include multi-tone, wideband frequency modulation (FM), and OFDM.
- `specsense.m` - This function performs energy detection based spectrum sensing and produces a REM for use in modifying the PN sequence. The output REM consists of a binary vector indicating channel availability.
- `codeGen.m` - This function reads in a list of available FH channels and generates the PN sequence. The function also produces the waveform used to mix the baseband signal up to the FH IF.
- `wl_init_txrx.m` - This script is used to initialize a transmit and receive board based on user specified parameters (such as the number of FH channels or chips per symbol). Board parameters such as sample frequency and symbol duration are packaged in an object `params` which may easily be passed to other functions.
- `wl_init_txrxix.m` - This script provides the same functionality as `wl_init_txrx.m` for three boards. These two scripts will be combined in a single function that will accommodate a variable number of radios.
- `wl_estNoise.m` - This function is used to estimate the average ambient noise power observed by the receiver. It can also be used to estimate how Gaussian the noise is.
- `wl_estSigPwr.m` - This function is used to estimate the signal power observed by the receiver.
- `wl_estInt.m` - Like `wl_estSigPwr.m`, this function is used to estimate the power observed by the receiver from the interfering transmitter.

- `wl_fsk_txrx.m` - This function provides a basic MFSK FH modem for use with WARPlab. The modulation order, the number of FH channels, and the number of chips per symbol are adjustable to determine the impact to BER. The function produces a plot of BER as a function of SNR or E_B/N_0 .
- `wl_spec_analyzer.m` - This function allows a board to be used as a limited functionality spectrum analyzer.
- `wl_snr.m` - This function provides the same capability as `wl_fsk_txrx.m` but includes a third board as an interfering transmitter.
- `wl_isr.m` - This function provides the same capability as `wl_snr.m` with the exception that BER is expressed as a function of ISR.
- `wl_dsa.m` - This function provides the same capability as `wl_fsk_txrx.m` with spectrum sensing and waveform adaptation enabled. BER is expressed as a function of the ratio of spectrum sensing rate to environment change rate.

References

- [1] J. Mitola and G. Maguire, "Cognitive Radio: Making Software Radios More Personal," *Personal Communications, IEEE*, vol. 6, no. 4, pp. 13–18, 1999.
- [2] S. Haykin, "Cognitive Radio: Brain-Empowered Wireless Communications," *Selected Areas in Communications, IEEE Journal on*, vol. 23, no. 2, pp. 201–220, 2005.
- [3] Air Force Chief Scientist, Office of the, *Report on Technology Horizons: A Vision for Air Force Science & Technology During 2010–2030*, pp. 52–55, 60, 78–91. 2010.
- [4] "Advanced RF Mapping (Radio Map)," *DARPA Strategic Technology Office*, 2012.
- [5] Z. Zhang, K. Long, and J. Wang, "Self-Organization Paradigms and Optimization Approaches for Cognitive Radio Technologies: a survey," *Wireless Communications, IEEE*, vol. 20, pp. 36–42, April 2013.
- [6] B. Wang and K. Liu, "Advances in Cognitive Radio Networks: A Survey," *Selected Topics in Signal Processing, IEEE Journal of*, vol. 5, no. 1, pp. 5–23, 2011.
- [7] R. Mclean, M. Silvius, K. Hopkinson, B. Flatley, E. Hennessey, C. Medve, J. Thompson, M. Tolson, and C. Dalton, "An Architecture for Coexistence with Multiple Users in Frequency Hopping Cognitive Radio Networks," *Selected Areas in Communications, IEEE Journal on*, vol. 32, no. 3, p. To appear, 2014.
- [8] R. McLean, B. Flatley, M. Silvius, and K. Hopkinson, "FPGA-Based RF Spectrum Merging and Adaptive Hopset Selection," in *Aerospace Conference, 2013 IEEE*, pp. 1–8, 2013.
- [9] R. McLean, M. Silvius, and K. Hopkinson, "Method for Evaluating k-Means Clustering for Increased Reliability in Cognitive Radio Networks," in *Software Security and Reliability (SERE), 2013 IEEE 7th International Conference on*, pp. 99–108, 2013.
- [10] R. C. Dixon, *Spread Spectrum Systems with Commercial Applications*. John Wiley & Sons, Inc., 1994.
- [11] A. De Domenico, E. Strinati, and M. Di Benedetto, "A Survey on MAC Strategies for Cognitive Radio Networks," *Communications Surveys Tutorials, IEEE*, vol. 14, no. 1, pp. 21–44, 2012.
- [12] W. Wang, "Spectrum Sensing for Cognitive Radio," in *Intelligent Information Technology Application Workshops, 2009. IITAW '09. Third International Symposium on*, pp. 410–412, 2009.

- [13] T. Yucek and H. Arslan, "A Survey of Spectrum Sensing Algorithms for Cognitive Radio Applications," *Communications Surveys Tutorials, IEEE*, vol. 11, no. 1, pp. 116–130, 2009.
- [14] W. Lin and Q. Zhang, "A Design of Energy Detector in Cognitive Radio Under Noise Uncertainty," in *Communication Systems, 2008. ICCS 2008. 11th IEEE Singapore International Conference on*, pp. 213–217, 2008.
- [15] T. Hanninen, J. Vartiainen, M. Juntti, and M. Raustia, "Implementation of Spectrum Sensing on Wireless Open-Access Research Platform," in *2010 3rd International Symposium on Applied Sciences in Biomedical and Communication Technologies (ISABEL)*, pp. 1–5, 2010.
- [16] "WARP Project, <http://warpproject.org>."
- [17] C. Jiang, Y. Li, W. Bai, Y. Yang, and J. Hu, "Statistical Matched Filter Based Robust Spectrum Sensing in Noise Uncertainty Environment," in *Communication Technology (ICCT), 2012 IEEE 14th International Conference on*, pp. 1209–1213, 2012.
- [18] M. Bkassiny, S. Jayaweera, Y. Li, and K. Avery, "Blind Cyclostationary Feature Detection Based Spectrum Sensing for Autonomous Self-Learning Cognitive Radios," in *Communications (ICC), 2012 IEEE International Conference on*, pp. 1507–1511, 2012.
- [19] K.-H. Lee, A. Mate, and I.-T. Lu, "Practical Implementation of Time Covariance Based Spectrum Sensing Methods Using WARP," in *Systems, Applications and Technology Conference (LISAT), 2011 IEEE Long Island*, pp. 1–5, 2011.
- [20] Y. Zeng and Y.-C. Liang, "Eigenvalue-Based Spectrum Sensing Algorithms for Cognitive Radio," *Communications, IEEE Transactions on*, vol. 57, no. 6, pp. 1784–1793, 2009.
- [21] D. Bhargavi and C. Murthy, "Performance Comparison of Energy, Matched-Filter and Cyclostationarity-Based Spectrum Sensing," in *Signal Processing Advances in Wireless Communications (SPAWC), 2010 IEEE Eleventh International Workshop on*, pp. 1–5, 2010.
- [22] Y. Zhao, L. Morales, J. Gaeddert, K. Bae, J.-S. Um, and J. Reed, "Applying Radio Environment Maps to Cognitive Wireless Regional Area Networks," in *New Frontiers in Dynamic Spectrum Access Networks, 2007. DySPAN 2007. 2nd IEEE International Symposium on*, pp. 115–118, 2007.
- [23] L. Iacobelli, P. Fouillot, and C. Le Martret, "Radio Environment Map Based Architecture and Protocols for Mobile Ad Hoc Networks," in *Ad Hoc Networking Workshop (Med-Hoc-Net), 2012 The 11th Annual Mediterranean*, pp. 32–38, 2012.

- [24] S. Faint, O. Ureten, and T. Willink, "Impact of the Number of Sensors on the Network Cost and Accuracy of the Radio Environment Map," in *Electrical and Computer Engineering (CCECE), 2010 23rd Canadian Conference on*, pp. 1–5, 2010.
- [25] Z. Wei, Q. Zhang, Z. Feng, W. Li, and T. Gulliver, "On the Construction of Radio Environment Maps for Cognitive Radio Networks," in *Wireless Communications and Networking Conference (WCNC), 2013 IEEE*, pp. 4504–4509, 2013.
- [26] V. Atanasovski, J. van de Beek, A. Dejonghe, D. Denkovski, L. Gavrilovska, S. Grimoud, P. Mahonen, M. Pavloski, V. Rakovic, J. Riihijarvi, and B. Sayrac, "Constructing Radio Environment Maps With Heterogeneous Spectrum Sensors," in *New Frontiers in Dynamic Spectrum Access Networks (DySPAN), 2011 IEEE Symposium on*, pp. 660–661, 2011.
- [27] D. Duan and L. Yang, "Cooperative Spectrum Sensing with Ternary Local Decisions," *Communications Letters, IEEE*, vol. 16, no. 9, pp. 1512–1515, 2012.
- [28] M. Tolson, C. Dalton, M. Silvius, E. Hennessey, C. Medve, J. Thompson, K. Hopkinson, and S. Azghandi, "Totally-Ordered, Reliable Multicast over Cognitive Radio Networks," in *System Sciences (HICSS), 2013 46th Hawaii International Conference on*, p. To appear, 2014.
- [29] C. Medve, M. Seery, M. Silvius, R. McTasney, and K. Hopkinson, "Hardware Implementation of Gold's Algorithm for Rendezvous in Adaptable FH Cognitive Radio Networks," in *SDR Wireless Innovation Forum*, p. To appear, 2014.
- [30] M. Song, J. Pennington, M. Silvius, R. Thomas, and R. Martin, "Design and Performance Tradeoffs in Digital Radio Processing Architectures," in *SDR '10 Technical Conference and Product Exposition, Proceedings of the*, pp. 282–287, 2010.
- [31] R. L. Peterson, R. E. Ziemer, and D. E. Borth, *Introduction to Spread Spectrum Communications*. Prentice Hall, 1995.
- [32] S. Haykin, *Communication Systems*. John Wiley & Sons, Inc., 2001.
- [33] B. Sklar, *Digital Communications: Fundamentals and Applications*. Prentice Hall, 2001.
- [34] G. R. Cooper and C. D. McGillem, *Modern Communications and Spread Spectrum*. McGraw Hill, 1986.
- [35] Y. Zhao, L. Morales, J. Gaeddert, K. Bae, J.-S. Um, and J. Reed, "Applying Radio Environment Maps to Cognitive Wireless Regional Area Networks," in *2nd IEEE International Symposium on New Frontiers in Dynamic Spectrum Access Networks, 2007. DySPAN 2007.*, pp. 115–118, 2007.

- [36] A. Viterbi, *Principles of Coherent Communications*. McGraw-Hill Book Company, 1966.

REPORT DOCUMENTATION PAGE					<i>Form Approved</i> OMB No. 0704-0188	
The public reporting burden for this collection of information is estimated to average 1 hour per response, including the time for reviewing instructions, searching existing data sources, gathering and maintaining the data needed, and completing and reviewing the collection of information. Send comments regarding this burden estimate or any other aspect of this collection of information, including suggestions for reducing this burden to Department of Defense, Washington Headquarters Services, Directorate for Information Operations and Reports (0704-0188), 1215 Jefferson Davis Highway, Suite 1204, Arlington, VA 22202-4302. Respondents should be aware that notwithstanding any other provision of law, no person shall be subject to any penalty for failing to comply with a collection of information if it does not display a currently valid OMB control number. PLEASE DO NOT RETURN YOUR FORM TO THE ABOVE ADDRESS.						
1. REPORT DATE (DD-MM-YYYY) 27-03-2014		2. REPORT TYPE Master's Thesis		3. DATES COVERED (From — To) Oct 2013–Mar 2014		
4. TITLE AND SUBTITLE Opportunistic Access in Frequency Hopping Cognitive Radio Networks				5a. CONTRACT NUMBER		
				5b. GRANT NUMBER		
				5c. PROGRAM ELEMENT NUMBER		
6. AUTHOR(S) Hennessey, Ethan S., Captain, USAF				5d. PROJECT NUMBER		
				5e. TASK NUMBER		
				5f. WORK UNIT NUMBER		
7. PERFORMING ORGANIZATION NAME(S) AND ADDRESS(ES) Air Force Institute of Technology Graduate School of Engineering and Management (AFIT/EN) 2950 Hobson Way WPAFB, OH 45433-7765				8. PERFORMING ORGANIZATION REPORT NUMBER AFIT-ENG-14-M-38		
9. SPONSORING / MONITORING AGENCY NAME(S) AND ADDRESS(ES) Dr. Vasu Chakravarthy 2241 Avionics Circle WPAFB, OH 45433 vasu.chakravarthy@us.af.mil 937-528-8269				10. SPONSOR/MONITOR'S ACRONYM(S) AFRL/RVWE		
				11. SPONSOR/MONITOR'S REPORT NUMBER(S)		
12. DISTRIBUTION / AVAILABILITY STATEMENT DISTRIBUTION STATEMENT A: APPROVED FOR PUBLIC RELEASE; DISTRIBUTION UNLIMITED						
13. SUPPLEMENTARY NOTES This work is declared a work of the U.S. Government and is not subject to copyright protection in the United States.						
14. ABSTRACT Researchers in the area of cognitive radio often investigate the utility of dynamic spectrum access as a means to make more efficient use of the radio frequency spectrum. Many studies have been conducted to find ways in which a secondary user can occupy spectrum licensed to a primary user in a manner which does not disrupt the primary user's performance. This research investigates the use of opportunistic access in a frequency hopping radio to mitigate the interference caused by other transmitters in a contentious environment such as the unlicensed 2.4 GHz region. Additionally, this work demonstrates how dynamic spectrum access techniques can be used not only to prevent interfering with other users but also improve the robustness of a communication system.						
15. SUBJECT TERMS Cognitive radio, dynamic spectrum access, opportunistic access, frequency hopping spread spectrum, energy detection						
16. SECURITY CLASSIFICATION OF:			17. LIMITATION OF ABSTRACT UU	18. NUMBER OF PAGES 72	19a. NAME OF RESPONSIBLE PERSON Dr. Kenneth M. Hopkinson (ENG)	
a. REPORT U	b. ABSTRACT U	c. THIS PAGE U			19b. TELEPHONE NUMBER (include area code) (937) 255-3636 x4579 kenneth.hopkinson@afit.edu	